# Sleep fragmentation after traumatic brain injury impairs behavior and conveys long-lasting impacts on neuroinflammation

Samuel Houle [a], Zoe Tapp [a,b], Shannon Dobres [a], Sakeef Ahsan [a], Yvanna Reyes [a], Christopher Cotter [a], Jessica Mitsch [a], Zachary Zimomra [b], Juan Peng [d], Rachel K. Rowe [e], Jonathan Lifshitz [f], John Sheridan [b,g], Jonathan Godbout [a,b,c], Olga N. Kokiko-Cochran [a,b,c,*]

[a] Dept. of Neuroscience, College of Medicine, The Ohio State University, 1858 Neil Ave, 43210, Columbus, OH, USA
[b] Institute for Behavioral Medicine Research, Neurological Institute, The Ohio State University, 460 Medical Center Drive, 43210, Columbus, OH, USA
[c] Chronic Brain Injury Program, The Ohio State University, 190 North Oval Mall, 43210, Columbus, OH, USA
[d] Center for Biostatistics, The Ohio State University, 320-55 Lincoln Tower, 1800 Cannon Drive, 43210, Columbus, OH, USA
[e] Department of Integrative Physiology, University of Colorado Boulder, Boulder, CO, USA
[f] Phoenix VA Health Care System and University of Arizona College of Medicine-Phoenix, Phoenix, AZ, USA
[g] Division of Biosciences, College of Dentistry, The Ohio State University, 305 W. 12th Ave, 43210, Columbus, OH, USA

A B S T R A C T

Traumatic brain injury (TBI) causes a prolonged inflammatory response in the central nervous system (CNS) driven by microglia. Microglial reactivity is exacerbated by stress, which often provokes sleep disturbances. We have previously shown that sleep fragmentation (SF) stress after experimental TBI increases microglial reactivity and impairs hippocampal function 30 days post-injury (DPI). The neuroimmune response is highly dynamic the first few weeks after TBI, which is also when injury induced sleep-wake deficits are detected. Therefore, we hypothesized that even a few weeks of TBI SF stress would synergize with injury induced sleep-wake deficits to promote neuroinflammation and impair outcome. Here, we investigated the effects of environmental SF in a lateral fluid percussion model of mouse TBI. Half of the mice were undisturbed, and half were exposed to 5 h of SF around the onset of the light cycle, daily, for 14 days. All mice were then undisturbed 15–30 DPI, providing a period for SF stress recovery (SF-R). Mice exposed to SF stress slept more than those in control housing 7–14 DPI and engaged in more total daily sleep bouts during the dark period. However, SF stress did not exacerbate post-TBI sleep deficits. Testing in the Morris water maze revealed sex dependent differences in spatial reference memory 9–14 DPI with males performing worse than females. Post-TBI SF stress suppressed neurogenesis-related gene expression and increased inflammatory signaling in the cortex at 14 DPI. No differences in sleep behavior were detected between groups during the SF stress recovery period 15–30 DPI. Microscopy revealed cortical and hippocampal IBA1 and CD68 percent-area increased in TBI SF-R mice 30 DPI. Additionally, neuroinflammatory gene expression was increased, and synaptogenesis-related gene expression was suppressed in TBI-SF mice 30 DPI. Finally, IPA canonical pathway analysis showed post-TBI SF impaired and delayed activation of synapse-related pathways between 14 and 30 DPI. These data show that transient SF stress after TBI impairs recovery and conveys long-lasting impacts on neuroimmune function independent of continuous sleep deficits. Together, these finding support that even limited exposure to post-TBI SF stress can have lasting impacts on cognitive recovery and regulation of the immune response to trauma.

## 1. Introduction

Traumatic brain injury (TBI) is an increasingly common healthcare challenge both in the United States and worldwide. Domestically, an estimated 3.8 million individuals suffer from a TBI each year in what has been dubbed a "silent epidemic" (Goyal and Yadav, 2020; Laskowski et al., 2015). Advancements in TBI detection and treatment have improved survival rates resulting in a population of individuals who may experience sequelae decades after initial injury (Faul and Coronado, 2015). This time presents an opportunity for other life events to

influence chronic outcomes. Beyond cognitive impairment, survivors may experience psychiatric complications and even neurodegeneration over time (Ahmed et al., 2017). Pre-clinical and clinical data suggest that there is a link between moderate TBI and future dementia presentation (Kokiko-Cochran and Godbout, 2018; Raj et al., 2022; Zyśk et al., 2019); however, the factors that link TBI to development of neurodegenerative disease remain unclear. Therefore, identifying and characterizing exogenous factors that complicate TBI recovery and worsen chronic outcomes are important areas of study.

Following TBI, reactive microglia resolve into a "primed" phenotype. When primed, pre-clinical studies show that microglia continue to express elevated markers for microglial reactivity, such as major histocompatibility complex class-II, CD11b, and Toll-like receptors (TLR), increase production of inflammatory cytokines IL-1β and IL-6, and display de-ramified morphologies with higher ionized calcium-binding adapter molecule 1 (IBA1) and CD68 expression (Cunningham et al., 2005; Henry et al., 2009; Norden and Godbout, 2013; Torres-Platas et al., 2014). Primed microglia have exaggerated responses to subsequent stimuli, such as an additional TBI, immune challenge, or stress (Bray et al., 2022; Fenn et al., 2014). Experimental models show that secondary immune challenges after TBI increase neuroinflammation and worsen pathology, possibly bridging the gap between TBI and neurodegeneration (Chen et al., 2008; Houle and Kokiko-Cochran, 2022; Kokiko-Cochran and Godbout, 2018; Sun et al., 2017). While microglial-driven neuroinflammation is a critical component of an appropriate CNS response to injury, microglia can remain reactive for years following injury, and lingering neuroinflammation can become maladaptive and lead to neuronal damage (DiSabato et al., 2016; Johnson et al., 2013; Witcher et al., 2021). These data show that the neuroimmune system is vulnerable to hyperactivity following TBI, and a secondary immune stimulus may be sufficient to substantially alter outcome.

Actualized or perceived challenges to homeostasis are referred to as "stress" (Walker et al., 2013). In response to these challenges, mechanisms generally referred to as stress responses seek to return the body to homeostasis. Microglia offer the most robust adaptive immune response to stimuli and are hypothesized to mediate many of the effects of stress on the brain. Both acute and chronic psychosocial stress have been previously found to induce microglial responses in the brain, typically characterized by enhanced IBA1 and cytokine expression (Hinwood et al., 2012; Wohleb et al., 2012; Woodburn et al., 2021). Preclinical studies have also found microglia become primed by stress, exhibiting exaggerated reactions to secondary challenge following a stress response (Frank et al., 2012). Therefore, stress alone can serve as a potent stimulator of microglial reactivity. Together, these findings support that microglia are highly involved in the regulation of stress responses and mediating the effects of stress in the CNS. Stress can therefore serve as a secondary source of microglial activation following TBI and complicate the chronic neuroinflammatory environment following injury.

For this manuscript, "sleep disruptions" will refer to the disruption of sleep via mechanical sleep fragmentation (SF) which is analogous to exogenous SF that TBI survivors can experience in clinical or home settings. "Sleep disturbances" will refer to alterations in sleep as a behavioral manifestation, that occur as a consequence of TBI pathology or subacute stress exposure. On their own, sleep disruptions are a potent source of stress and disrupt proper hypothalamus-pituitary-adrenal axis function (Hirotsu et al., 2015; Medic et al., 2017). However, perceived stress is also highly associated with sleep disturbances. Therefore, a powerful bidirectional relationship exists between sleep and stress, and TBI survivors may be particularly vulnerable to the detrimental effects of sleep disturbance. TBI induces a variety of sleep disturbance such as insomnia, excessive daytime sleepiness, and dysfunctional rapid eye movement (REM) sleep (Wickwire et al., 2016). In fact, as many as half of all TBI survivors report experiencing some form of sleep disturbance following TBI (Chan and Feinstein, 2015; Mathias and Alvaro, 2012). Populations susceptible to sleep disturbances have more perturbed sleep

in response to stress (Drake et al., 2017; Peterson et al., 2008). For example, stress-induced sleep disturbances are prevalent in TBI survivors and are tied to worsened outcome (Kalmbach et al., 2018a, 2018b). Therefore, stress- and injury-induced sleep disturbances could synergize to influence recovery. We predict that inflammation, through microglial activation, is instrumental in this process.

We have previously shown that 4 h of daily post-TBI SF stress exaggerates microglial responses and impairs neuronal function within the hippocampus 30 days post-injury (DPI) (Tapp et al., 2022). Additionally, we have shown that chronic post-TBI SF stress results in lasting blood brain barrier disruption and transcriptional changes indicative of impaired neuronal maintenance and excitability 60 DPI (Tapp et al., 2023). Temporal change in the inflammatory response to experimental TBI provides an opportunity to examine whether the injured brain is particularly vulnerable to secondary immune stimulus during discrete phases. Work by Izzy et al. found that the acute response to TBI was marked by elevated proinflammatory gene expression that began to resolve by the sub-acute 14 DPI time point (Izzy et al., 2019). Thus 14 DPI was identified as a pivotal transition between the subacute and chronic TBI response. The present study expands on our previous findings by investigating whether SF stress limited to the sub-acute post--injury phase (1–14 DPI) imparts lasting alterations in sleep, microglial reactivity, and transcriptional regulation of neuroinflammation at the chronic 30 DPI time point. We effectively targeted the period of transition where mouse sleep is increased the most by extending daily SF exposure to 5 h from Zeitgeber (ZT) 23–4. For the first time in a model of post-TBI SF stress, we determined sleep-wake behavior 1–30 DPI with non-invasive homecage activity recordings. Using Morris Water Maze (MWM) we determined the effect of post-TBI SF stress on sub-acute spatial memory and inflammatory outcomes were measured by cortical RNA expression analysis and IBA1/CD68 immunolabeling. We found that 14 days of SF stress after TBI impairs recovery and conveys long-lasting impacts on neuroimmune function independent of continuous sleep deficits 30 DPI. Together, these studies highlight that even transient SF stress after TBI can have lasting implications for chronic TBI sequelae and recovery.

## 2. Methods

### 2.1. Mice and sourcing

Equal numbers of 8–10 week-old male and female C57BL/6 mice (n = 99) from Charles River Laboratories (Wilmington, MA) were used in these experiments. Mice were group-housed and separated by sex in the Ohio State University Laboratory Animal Resource (ULAR). Mice were granted *ad libitum* access to food and water and were maintained under constant temperature (72–76 °F) and humidity with a 12:12 h light/dark cycle (Light onset, 6am = ZT 0). These experiments used a lateral fluid percussion model of TBI. To control for injury effects sham injuries were performed. All mice were subjected to one of two injury conditions: sham, and TBI. We used mechanical SF as a model of environmental stress. All mice were housed under one of two sleep conditions: control (CON), and SF. Upon reaching the designated endpoints, mice were euthanized by $CO_2$ asphyxiation followed by either transcardial perfusion with phosphate buffered saline (PBS) or rapid decapitation. Perfused brains were removed and drop-fixed in 4% paraformaldehyde (PFA) for histochemical analysis. Decapitated brains were removed on ice and micro-dissected to obtain injured cortical tissue which was snap-frozen in liquid nitrogen for future RNA analysis. All conditions described were in accordance with the National Institutes of Health Guidelines for the Care and Use of Laboratory Mice and approved by the Institutional Animal Care and Use Committee at the Ohio State University.

## 2.2. Experimental design

This study employed a 2 (Sham, TBI) × 2 (Control, SF) factorial design to investigate how post-TBI SF stress alters recovery from injury. Mice received either a moderate lateral fluid percussion TBI or a sham injury. Following injury, mice were randomly selected and evenly divided to either be housed in control conditions, or to receive daily post-injury mechanical SF 1–14 DPI. Behavioral testing was completed 7 DPI (Open field test and Y maze) and 9–14 DPI (Morris Water Maze). At 15 DPI, all mice were placed in control housing. Upon reaching 30 DPI, brains were collected for histological analysis. Mice receiving sleep monitoring (Signal Solutions LLC, Lexington, KY) were singly housed and did not complete behavioral testing to minimize recording disruptions. Gene expression in the cortex was evaluated in mice that received sleep monitoring well as a subset of mice aging 14 DPI that did not complete behavioral testing.

## 2.3. Statistics

For all experiments appropriate sample sizes were determined based on previous studies (Bray et al., 2022; Tapp et al., 2020, 2022). For most sleep, behavioral, and histochemical data, 2-way analysis of variance (ANOVA) was conducted in Graphpad 8 (Prism). For comparisons with repeated measures, 3-way ANOVAs were conducted in SPSS (IBM). In these repeated measure ANOVAs, sphericity was not assumed and Greenhouse-Giesser corrections were used to limit Type 1 error rates. In the Morris water maze where sex effects were observed, we utilized mixed effects models to test the injury and sleep effect on latency. Fixed effects included day, injury group, sleep condition, and their interaction. Of primary interest were preplanned contrasts comparing group means at each of the 5 time points. Random effect included a subject-specific random intercept to account for within-subject correlation (repeated time points). The Kenward-Roger adjustment to the degrees of freedom was used to control Type I error rates. Sleep bout data were measured with multivariate regression to measure the degree to which vectors of different dependent variables are aligned to each other. Two-sided significance of $\alpha = 0.05$ was used for mixed effect and multivariate regression analysis. Analyses were performed in SAS version 9.4 (SAS institute, Cary, NC). For Nanostring nCounter data, we obtained normalized gene counts using the DESeq2 package in R and used SPSS to perform 2-way ANOVA to identify genes with counts significantly altered by group. Bonferroni *post hoc* analysis was performed when interaction effects were detected in experiments without repeated measures. Tukey *post hoc* analysis was performed for comparisons with repeated measures. For pathway analysis, right-tailed Fischer's exact test with Benjamini-Hochberg corrections for multiple hypothesis was used to compare differences between groups of interest. All comparisons with $p < 0.05$ were reported. For all experiments and data processing, researchers were blind to animal group identification.

## 2.4. Surgical preparation and lateral fluid percussion injury (FPI)

Surgical preparations were completed as previously described (Fitzgerald et al., 2022; Tapp et al., 2020, 2022, 2023). Briefly, mice were anesthetized with 4% isoflurane gas for 4 min. Mice were then shaved along the top of their head, fixed in a stereotaxic frame, and sterilized. An incision was made at the midline of their skull and fascia was cleared away to allow access to the skull. Then, a drill was used to create a small guide notch on the right parietal bone approximately 4 mm to the right of midline, directly between lambda and bregma. This notch served as a guide for a trephine drill which was used to perform a 3 mm craniectomy over the parietal lobe while leaving the dura intact. Once the skull flap was removed, a modified luer-lock syringe, modified to be about 1 cm tall with an internal diameter of 3 mm, was affixed to the craniectomy using super glue and sealed using dental cement. The hub was then filled with saline, and mice were injected with 2 ml of saline subcutaneously before being removed from the stereotaxic and returned to their homecage.

The following day, mice were again anesthetized using 4% isoflurane for 4 min. At the end of the 4 min the hub was filled with saline and mice were subsequently attached to a fluid percussion injury (FPI) device (Custom Design & Fabrication, Richmond, VA). To induce a moderate injury, a weighted pendulum from a pre-set height was released, creating a fluid pulse that compressed the exposed dura. The pressure of the fluid pulse was maintained at 1 atm. Following injury induction, hubs were removed and the incision was closed by staples. Half of the mice were randomly selected to receive this injury. For the sham population, mice were anesthetized and affixed to the FPI device but did not receive a fluid pulse. They then immediately had their hubs removed and incisions closed. All mice had their injury severity assessed by measuring their latency to self-righting reflex following TBI or sham injury.

## 2.5. Sleep fragmentation stress

Following injury half of all TBI and sham mice were randomly selected to receive daily, mechanical SF or be left undisturbed. Mechanical SF was provided automatically every 2 min from ZT 23–4, 1–14 DPI using specialized SF chambers (Lafayette Instruments). SF protocols were adapted from our previous studies (Tapp et al., 2022, 2023). Control mice were housed in the same room but were not exposed to SF stress for the duration of the study. For all studies, mice were group housed in SF or control housing except for studies using piezo-electric sleep monitoring in which case mice were singularly housed. Following the 14 days of SF stress, all mice received control housing in which half of the mice were allowed to recover without SF stress until 30 DPI. Therefore, data from 15-30 DPI are designated as SF-Recovery (SF-R).

## 2.6. Piezoelectric sleep recordings

Custom-molded piezoelectric sensors were used to measure mouse sleep 1–30 DPI (Signal Solutions LLC, Lexington, KY). Previous iterations of these sensors have been demonstrated to classify sleep behavior based on physiological parameters and have been validated against EEG and human observations with >90% accuracy (Donohue et al., 2008). Mice were introduced to the cages immediately following injury and were left undisturbed except for daily wellness checks. 30 DPI mice were removed for tissue collection. Data were analyzed using SleepStats2p18 (Signal Solutions, Lexington, KY). Piezoelectric signals were analyzed over 8 s epochs and decision statistics were calculated utilizing regular amplitude signals recorded during the epoch. Regular beathing at 2–4 Hz was classified as sleep-behavior which was differentiated from quiet and active wake at higher frequencies (Donohue et al., 2008). Percent-sleep data were exported in bins of 1 h to allow for averaging of discrete time periods. Minimum sleep bout epoch length was set to 4 s. Total number of sleep bouts was exported in histograms for the light and dark periods of each day. Sleep bout lengths were binned by multiplying increments of 4 s and resulted in 8 bins (4–8 s, 8–16 s, 16–32 s, 32–64 s, 64–128 s, 128–256 s, 256–512 s, and 512+ s). Observed sleep bouts were sorted into appropriate bins by their length. Total number of sleep bouts within each bin was reported for each subject over a given period of time and were then averaged per experimental group. For percent-sleep and sleep bout data from 1 to 14 DPI hours ZT 23–4 were removed from analysis to avoid signal artifact from the mechanical SF.

## 2.7. Behavioral assessment

All Behavioral testing was performed in the Ohio State College of Medicine's Behavioral Core. Paradigms were adapted from previously validated protocols routinely performed by the Behavioral Core. For each day of behavioral testing mice were removed from their housing at

ZT 13, 1 h following the onset of the mice's dark cycle and staged outside of the behavioral testing room for 1 h to allow for acclimation. Testing began at ZT 14. All acclimation and testing were conducted under red light.

### 2.7.1. Open field test

An open field analysis assessed motor and anxiety-like behavior. Open field testing was performed as previously described (Tapp et al., 2022). During the dark period 7 DPI, mice were gently placed facing the corner of a plexiglass chamber and permitted to investigate for 10 min. The time spent in the center and periphery, and the total distance traveled, were recorded using floor-level light beams that can track mouse position in the maze (San Diego Instruments). The chamber was sanitized with 70% ethanol between animal sessions.

### 2.7.2. Y maze

Y-maze testing was used to analyze spatial-working memory as previously described (Kokiko-Cochran et al., 2018). During the dark period 7 DPI and after open field analysis, mice were allowed to freely explore a three-armed Y-maze apparatus for 5 min. Between mice, the maze was cleaned using 70% ethanol. The total arm entries and spontaneous alternations were scored by a blinded investigator. The spontaneous alternation scoring criteria included three sequential arm entries into separate arms labeled 1–3. Data were analyzed as maximum percent spontaneous alternations of (total entries - 2).

### 2.7.3. Morris Water Maze

Morris water maze (MWM) was used to measure spatial learning and memory 9–14 DPI. MWM protocols were adapted from previous paradigms (Kokiko-Cochran et al., 2018). Procedural learning was measured in four test trials via visible platform training. During visible platform training, a 4 ft diameter tub was filled with water so that the top of an escape platform was exposed. A visual cue (black conical) was attached to the platform. The mice were placed in the tub at one of the four starting positions and allowed 60 s to locate the platform. Mice successful in finding the platform were left there for 15 s before being removed from the tub by the investigator. Mice unsuccessful in 60 s were guided towards the platform and left there for 15 s before being removed. The trials were repeated for each of the remaining three starting locations. All testing occurred during the dark periods of the respective days to avoid further disruption of mouse sleep during the light (active) period.

For days 2–6 of testing, the tub was filled with water, and made opaque by adding non-toxic white paint, to cover the top of the platform and the visual cue removed. The mice underwent the same procedure consisting of four trials during each day but needed to rely on spatial cues outside of the maze to locate the submerged platform. Starting positions were randomized across each day. Mice had a maximum of 60 s per trial to reach the platform. If the mouse reached the platform, they were allowed to remain for 15 s before removal. If mice failed to find the platform they were guided to its location and removed after 15 s. Care was taken to minimize noise or visual confounds and the maze was cleaned between trials.

### 2.8. RNA isolation and nanostring nCounter glial profiling

Brains were collected via rapid decapitation 14 and 30 DPI. RNA was obtained and processed for nCounter analysis as previously described (Tapp et al., 2022, 2023). Injured cortex was rapidly dissected on ice and then snap frozen in liquid nitrogen and stored at $-80\,^{\circ}C$. Frozen cortices were added to Trizol and RNA was isolated using the Tri-Reagent protocol (Sigma-Aldrich). RNA concentration and quality was recorded using a Nanodrop spectrophotometer (Fischer Scientific). RNA transcripts were then quantified by the OSUCCC Genomics Shared Resource facility (OSU) using nCounter analysis aligned to the Glial Profiling Panel (NanoString Technologies). The Glial Profiling panel screens for 700+ genes all involved with components of glial cell functioning in the brain. Counts were normalized using the DESeq2 Bioconductor package in R. Analysis of altered upstream regulator function of downstream canonical pathways was performed using Ingenuity Pathway Analysis (IPA) (Qiagen Inc.). Enriched pathways were analyzed using Comparison Analysis. In this analysis differentially expressed genes (DEG) between each condition and the sham control conditioned are considered to determine whether particular pathways are significantly activated or inhibited.

### 2.9. Immunofluorescence histochemistry (IF)

The isolated brains were perfused, dissected, and post-fixed in 4% PFA for 48 h then stored in 30% sucrose for 72 h at $4\,^{\circ}C$. Brain tissue was sectioned at 30 μm via a Leica CM1800 cryostat (Leica Biosystems) and transferred into cryoprotectant (30% ethylene glycol, 30% polyethylene glycol, 40% 0.2 M PBS) at $-20\,^{\circ}C$ until staining. The sections were washed with 0.1% Triton X-100 in PBS (PSBT) and blocked (5% normal donkey serum, 0.3% Triton X-100 in PBS) at room temperature for 2 h. The sections incubated overnight in primary antibody with constant rotation at $4\,^{\circ}C$: rabbit anti-IBA1 (1:500 Wako), rat anti-CD68 (1:500, Abcam), goat anti-GFAP (1:500, Abcam), and rat anti-CD45 (1:500, Bio-Rad). The tissue was washed with PBST and incubated in fluorochrome-conjugated secondary antibody for 1 h at room temperature with rotation: donkey anti-rabbit 647 (IBA1, 1:1000, Invitrogen), donkey anti-rat 488 (CD68, 1:1000, Invitrogen), Donkey anti-goat 647 (GFAP, 1:1000, Invitrogen), Donkey anti-rat 594 (CD45, 1:1000, Invitrogen). The sections were mounted and coversliped using Fluoromount-G (Invitrogen). IBA1/CD68 co-labeled slides were imaged using a Leica DM6 CS upright confocal microscope at 20x magnification. 2–4 images were taken per region of interest for each animal. Images were taken as sequential z-stacks every 2 μm resulting in 8–12 images per stack depending on brain region. Defined regions of interest include the lateral primary somatosensory cortex, beginning at the ventral end of the lesion and extending to the lateral edge of the cortex, and the hippocampal CA1 field, beginning at the medial edge of the CA2 and the dorsal edge of the CA1. GFAP and CD45 images were acquired using an EVOS FL Auto 2 Imaging System (Thermo Fisher Scientific) using a 10x objective with 2–4 images taken per region of interest.

### 2.9.1. Image quantification

All IF quantification was performed using FIJI (Schindelin et al., 2012). Co-labeled IBA1/CD68 images were stacked in maximum intensity projections. A blinded investigator determined the percent-area of IBA1 by using manual thresholding to consistently capture the microglial somas and processes between sections. Microglial CD68 expression was determined by calculating the percent area of CD68/IBA1 colocalization. CD68/IBA1 colocalization was conducted by manually thresholding CD68 and IBA1 images separately. Binary masks of the positive staining were obtained for each image and overlayed using the multiply feature in the FIJI image calculator. This produced a single mask representing the portions of the image that were positive for both IBA1 and CD68. Percent-area of this mask was calculated and reported as percent-area CD68+/IBA1+. Final percentages reflect the amount of microglial-specific CD68 expression per image. GFAP percent-area was calculated from single-plane bright field images. Thresholding was performed by blinded investigators. Cells expressing CD45 were counted by hand by blinded investigators. Total numbers of CD45$^+$ cells reflect the number of cells present in a 10x image of the lesion penumbra excluding any infiltration past the corpus callosum or any cells present of the edge of the tissue to capture cells fully infiltrating into the cortex as previously described (Tapp et al., 2022).

## 3. Results

### 3.1. TBI decreases sleep and SF increases number of sleep bouts during dark period 1–7 DPI

We sought to determine whether 14 days of post-TBI SF stress would convey persistent changes in TBI pathophysiology 30 DPI. Mice were randomly assigned to 1 of 4 groups (Sham CON, Sham SF, TBI CON, TBI SF), as previously described (Fig. 1A). Time to regain righting reflex (righting time) was measured following the administration of the TBI or sham injury; TBI increased righting time (Injury, $F (1, 42) = 79.70, p < 0.05$; Fig. 1B). Mouse sleep was recorded and analyzed to study the effects of TBI and SF on sleep 1–30 DPI. Days were divided into the light (ZT 0–11) and dark period (ZT 12–23) to test whether effects were unique to mice inactive or active periods, respectively. The 5 h between ZT 23–4 were removed from analysis to avoid artifacts from mechanical SF 1–14 DPI. We found that changes in sleep-wake behavior were concentrated to the dark periods of mice when they are typically most active. Hourly percent-sleep during the dark period was averaged between 1 and 7 DPI (Fig. 1C). We also averaged daily dark period percent-sleep to see if there was a building effect of SF stress over time (Fig. 1D). Lastly, we averaged total dark period percent-sleep between 1 and 7 DPI (Fig. 1E). Percent-sleep did not change between hours (Fig. 1C) or days (Fig. 1D) within the dark period 1–7 DPI. TBI decreased total percent time sleeping 1–7 DPI (Injury, $F (1, 24) = 5.329, p < 0.05$; Fig. 1E). Next, number of sleep bouts within discrete bins were measured and plotted in a histogram for the total dark period (Fig. 1F). Number and length of sleep bouts were used to determine if TBI or SF affected the ability to properly regulate maintenance of sleep. No overall changes in sleep bout lengths were observed (Fig. 1F). However, bouts of particular lengths were affected by either SF or TBI. SF increased the number of 16–32 (SF, $F (1, 22) = 5.235, p < 0.05$; Fig. 1G), and 32–64 s sleep bouts (SF, $F (1, 22) = 4.437, p < 0.05$; Fig. 1H). These results show that post-injury SF causes fragmented sleep with an increased number of shorter sleep bouts compared to control groups. TBI decreased the number of 256–512 s sleep bouts (Injury, $F (1,22) = 8.136, p < 0.05$; Fig. 1I). Together, these data show that moderate TBI decreases total sleep during the dark period by preventing the consolidation of sleep into longer bouts while SF produces mild fragmentation of sleep during the dark period.

### 3.2. TBI prevents SF-Dependent increases in sleep bouts 8–14 DPI

Next, we sought to observe how SF stress impacts sleep during the sub-acute phase of TBI 8–14 DPI. As previously described, we calculated hourly (Fig. 2A), daily (Fig. 2B), and total (Fig. 2C) dark period percent-sleep 8–14 DPI. Together, there was no interaction effect between SF stress or injury and time when analyzing individual hours (Fig. 2A) or days (Fig. 2B). However, SF stress did increase hourly (Fig. 2A), and daily (Fig. 2B) dark period percent-sleep (SF, $F (1, 22) = 13.17, p < 0.05$; Fig. 2A-B). Additionally, SF increased total percent-sleep during the dark period (SF, $F (1, 22) = 13.17, p < 0.05$; Injury x SF, $F (1, 22) = 5.160, p < 0.05$; Fig. 2C). Post hoc comparisons revealed total dark period percent-sleep increased in sham SF and TBI SF mice, but not TBI control mice when compared to sham controls (Bonferroni, $p < 0.05$; Fig. 2C). These data show that there was a strong SF effect between 8 and 14 DPI where mice that received SF slept more than sham mice in the control condition. Next, sleep bout lengths during the dark period were plotted in a histogram, as previously described (Fig. 2D). Overall, SF increased the number of sleep bouts during the total dark period (SF, $F (1, 22) = 6.441, p < 0.05$; Fig. 2D). Individual bins were compared to ascertain whether bouts of particular lengths were affected by injury or SF. Post hoc analysis showed sham SF mice had more sleep bouts in the 16–32s (SF, $F (1, 22) = 4.944, p < 0.05$; Injury x SF, $F (1, 22) = 5.008, p < 0.05$; Bonferroni, $p < 0.05$; Fig. 2E) and 32–64 s bins (SF, $F (1, 22) = 10.17, p < 0.05$; Injury x SF, $F (1, 22) = 6.766, p < 0.05$; Bonferroni, $p < 0.05$; Fig. 2F) than sham control mice. Sham SF mice had more long sleep bouts lengths 64–128 s (SF, $F (1, 22) = 12.52, p < 0.05$; Injury x SF, $F (1, 22) = 6.200, p < 0.05$; Bonferroni, $p < 0.05$; Fig. 2G) and 128–252 s (SF, $F (1, 22) = 11.87, p < 0.05$; Injury x SF, $F (1, 22) = 6.300, p < 0.05$; Bonferroni, $p < 0.05$; Fig. 2H) than sham control mice. Lastly, in longer sleep bouts of 252–512 s SF mice engaged in more of these sleep bouts than control mice, regardless of injury (SF, $F (1, 22) = 8.887, p < 0.05$; Fig. 2I). Similar effects were not observed in TBI SF mice compared to any groups. Additionally, no differences in percent sleep were observed between groups during the light-period 8–14 DPI (Supplementary Fig 1A-C). No main effects or TBI × SF interaction effects were observed in the total sleep bout data (S Fig. 1D). however, a main effect of SF is observed representing a decrease in 8–16 s light period sleep bouts 8–14 DPI (SF, $F (1,22) = 6.397, p < 0.05$; S. Fig. 1E) Together, these data indicate that sham SF but not TBI SF mice may be able to compensate for two weeks of SF by increasing percent time sleeping during their dark period when mice are typically more active.

### 3.3. Post-injury SF stress induces sex specific impairments in Morris Water Maze 14 DPI

We assessed anxiety-like behavior in the open field test (OFT) 7 DPI (Fig. 3A-B). There was a main effect of SF on the distance that mice traveled within the OFT. Mice exposed to SF stress traveled the least distance while TBI did not affect distance traveled in the open field (SF, $F (1, 42) = 4.213, p < 0.05$; Fig. 3A). However, there were no differences in the amount of time spent in the center of the OFT (Fig. 3B). Next, we assessed spatial working memory using the Y maze 7 DPI. There were no differences observed in either spontaneous alternations or in total number of arm entries (Fig. 3C-D). Finally, we assessed spatial learning and memory using the MWM 9–14 DPI. Mice were given one day of visible platform training followed by five days of hidden platform testing. No differences were observed between groups during this day of training. Latency to escape was the primary dependent variable of interest (Fig. 3E-F). An interaction between sex, injury, and SF was found in latency to reach the submerged platform (Interaction, Sex × Injury × SF, $F (1, 37) = 5.98, p < 0.05$), therefore, sexes were analyzed separately. Within male mice, TBI and SF interacted to impair MWM performance (Interaction, Injury x SF, $F (1, 18) = 7.689, p < 0.05$; Fig. 3E). Male TBI SF mice had longer latencies to escape compared to TBI control mice 12 and 13 DPI (Tukey, $p < 0.05$; Fig. 3E). Female mice displayed no differences between groups (Fig. 3F). Differences in latency to escape were not due to any difference in swim speed between groups (Fig. 3G).

To assess learning within the MWM, mouse swim patterns were tracked across days and assigned to one of nine search strategy characterizations, as previously described (Brody and Holtzman, 2006; Kokiko-Cochran et al., 2018) (Fig. 3H). Search strategies could fall broadly into either looping, non-spatially directed, or spatially directed categories. Qualitatively, we observed that sham control, sham SF, and TBI control groups all decreased the percentage of random search strategies between the days of testing (Fig. 3I-L). To evaluate whether mice were using more accurate search strategies on the final day of testing we summed the total number of each strategy used 14 DPI. TBI SF mice increased the usage of non-spatially directed search strategies compared to TBI controls (Injury x SF, $F (1, 42) = 5.542, p < 0.05$; Fig. 3M). TBI SF mice also used more non-spatially directed search strategies than TBI control mice (Bonferroni, $p < 0.05$; Fig. 3M). Specifically, we observed that TBI SF mice used random search strategies more than TBI control mice on the final day of testing in the MWM (Interaction, Injury x SF, $F (1, 42) = 5.891$, Bonferroni, $p < 0.05$; Fig. 3N). No sex specific differences in search strategy were identified. Together, these data show that post-TBI SF stress induces sex specific deficits in latency to escape the MWM. Further, TBI SF mice of both sexes used more nonspatial and random search strategies than TBI control mice supporting that post-TBI SF stress impairs performance in the MWM.
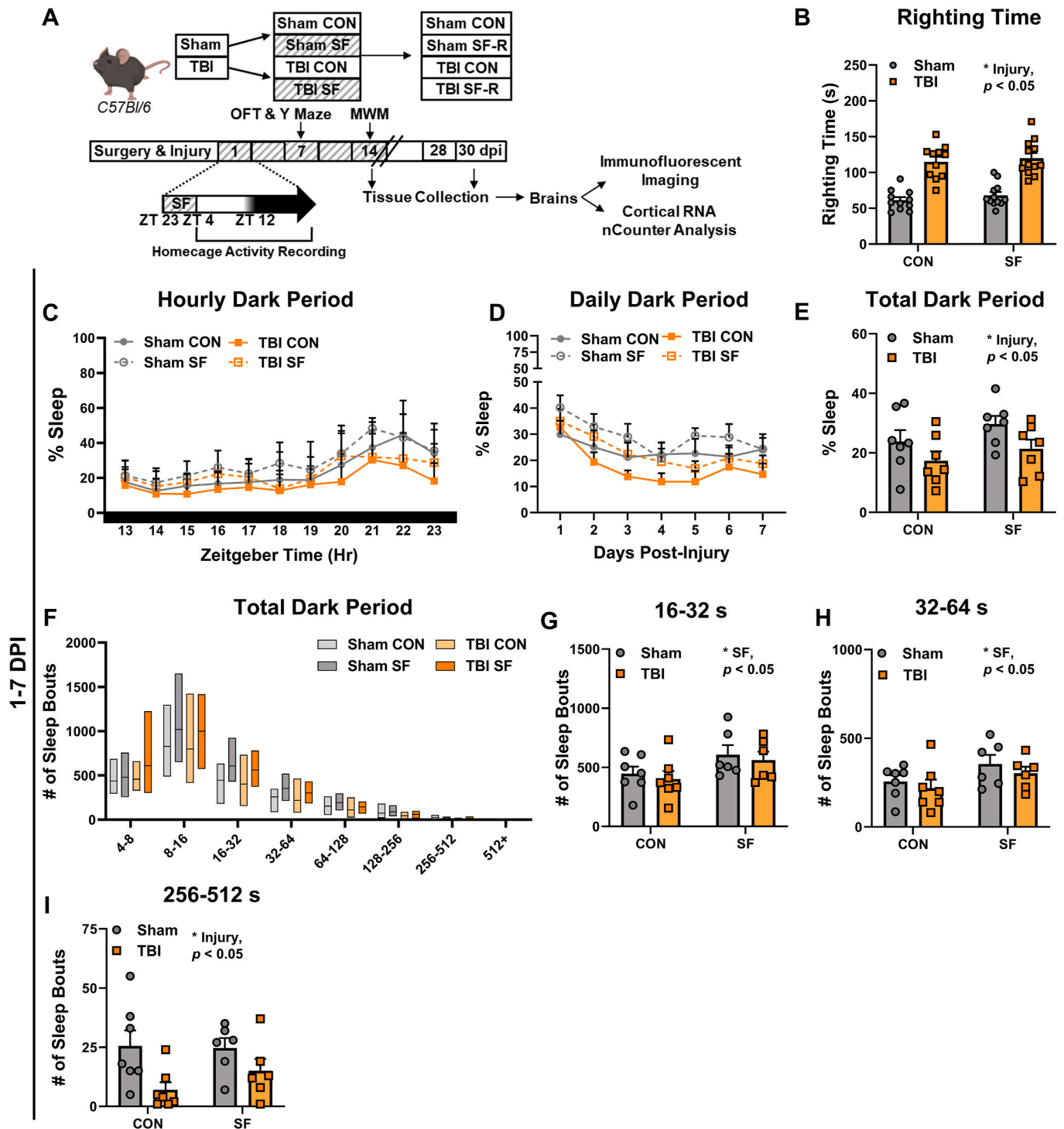
**Fig. 1. TBI decreases dark period sleep and SF stress fragments dark period sleep 1-7 DPI.** (A) Adult C57BL/6 mice received either lateral fluid percussion injury, or sham injury. Following injury, mice were housed in sleep fragmentation (SF) chambers for either 14 or 30 days post injury (DPI). TBI and sham mice either received 5 h of mechanical SF daily from 5am to 10am for the first 14 DPI and then recovered until 30 DPI or did not receive SF as control groups. Sleep was recorded by custom built nonintrusive piezoelectric sensors. Ipsilateral cortices were collected at 14 DPI for RNA analysis via Nanostring nCounter Glial Profiling Panels. Behaviors were assessed 7 DPI (OFT, Y maze), and 14 DPI (MWM) to track functional recovery from TBI. (B) TBI increased righting reflex times (Injury, $p < 0.05$). Time spent asleep and length of sleep bouts are recorded by piezoelectric sensors. (C) Hourly percent-sleep from the dark period averaged from 1 to 7 DPI showed no differences between groups. (D) Daily percent-sleep from the dark period 1–7 DPI showed no differences between groups within a particular day. (E) Total percent-sleep data was collapsed during the dark period over the first week of SF exposure. TBI decreased the percent-sleep mice engaged in during the dark period 1–7 DPI (Injury, $p < 0.05$). (F) Sleep bouts from the total dark period of each day 1–7 DPI were measured and sorted into bins depending on length. SF stress increased the number of sleep bouts that mice engaged in between (G) 16–32 s, and (H) 32–64 s. (I) TBI decreased the amount of longer sleep bouts 256–512 s that mice engaged in. (Mean ± SEM) (Percent-sleep = Mean ± SEM, Sleep bouts = Mean ± max/min).
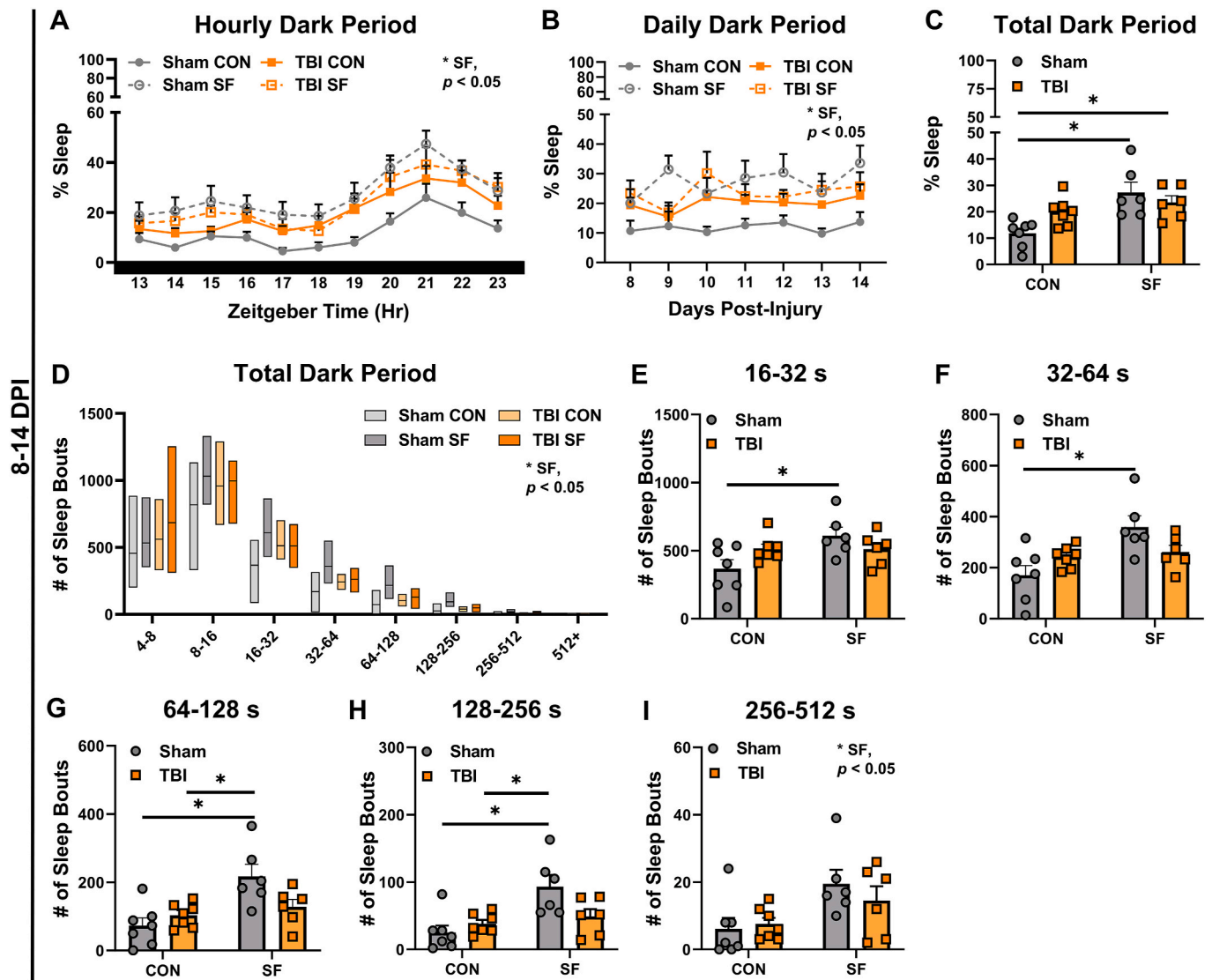
**Fig. 2. TBI prevents SF-dependent increases in sleep bouts 8-14 DPI.** We continued to measure sleep from 8 to 14 DPI during the second week that mice were exposed to SF. We found that changes to sleep were isolated to the dark period of each day. (A) We averaged each hour 8–14 DPI to show percent-sleep during each ZT hour of the dark period and found that SF increased percent-sleep (SF, $p < 0.05$). (B) When looking at daily averages for the entire dark period we found the same main effect where SF increased percent-sleep during the dark period and there is also a day by injury interaction effect where TBI increases percent-sleep specifically 10 DPI (Day x Injury, $p < 0.05$). (C) Next, we averaged total percent-sleep across 8–14 DPI. Injury and SF interacted to increase percent-sleep in both sham SF and TBI SF mice compared to sham control (Injury x SF, $p < 0.05$). (D) Next, we analyzed average number of sleep bouts from the total dark period 8–14 DPI. Sham SF mice engaged in more 16–32s (SF, $p < 0.05$; Injury x SF, $p < 0.05$; E) and 32–64s (SF, $p < 0.05$; Injury x SF, $p < 0.05$; F) sleep bouts than sham control. Sham SF mice engaged in more 64–128s (SF, $p < 0.05$; Injury x SF, $p < 0.05$; G) and 128–252s (SF, $p < 0.05$; Injury x SF, $p < 0.05$; H) sleep bouts than both sham control and TBI control mice while TBI SF mice were not significantly changed from any group. (I) In longer sleep bouts of 252–512s SF increased the number of sleep bouts mice engaged in during the dark period (SF, $p < 0.05$). (Percent-sleep = Mean ± SEM, Sleep bouts = Mean ± max/min).

### 3.4. 14 Days of post-injury SF stress does not affect sleep patterns 15–30 DPI

Mechanical SF was terminated 15 DPI, which provided a potential period of stress recovery between 15 and 30 DPI for TBI and sham mice exposed to SF. No differences in hourly or daily percent-sleep were detected between groups 15–21 DPI (Fig. 4A-B). Additionally, no differences in number and length of sleep bouts were observed between experimental groups during the light (Fig. 4C) or dark period (Fig. 4D) 15–21 DPI. Consistent with the first week of SF-R, no differences in hourly or daily sleep (Fig. 4 E-F), or number of sleep bouts (Fig. 4G-H) were detected 22–29 DPI. Together, these data show that chronic sleep deficits are not detected in this model of LFPI. Also, a period of recovery is sufficient to normalize sleep-wake behavior following daily post-injury SF stress.

### 3.5. SF stress increases inflammatory signaling in TBI mice 14 DPI

Next, we isolated RNA from the injured cortex 14 DPI and used a Nanostring glial profiling nCounter panel to assess the inflammatory response to TBI and SF. To determine the overall effect of TBI, we compared TBI controls to sham controls and TBI SF mice to sham SF mice and identified the genes that were uniformly increased or decreased in both comparisons (Fig. 5A). This yielded 41 genes that constitute the overall effect of TBI. These 41 genes were sorted by their roles as identified by Nanostring and the roles with the most altered genes include "neurogenesis" and "primed microglia". Both neurogenesis (*Ascl4, Atp8a2, Etv5, Hmgb1, Lrrc7, Nrcam, Opcml*, and *Stat3*) and primed microglia (*Atp8a2, C3, Ccr5, Ckb, Cybb, Eid1, Lgals3*, and *Slc24a3*) related genes were increased as an overall effect of TBI compared to sham groups. The overall effect of SF stress was also
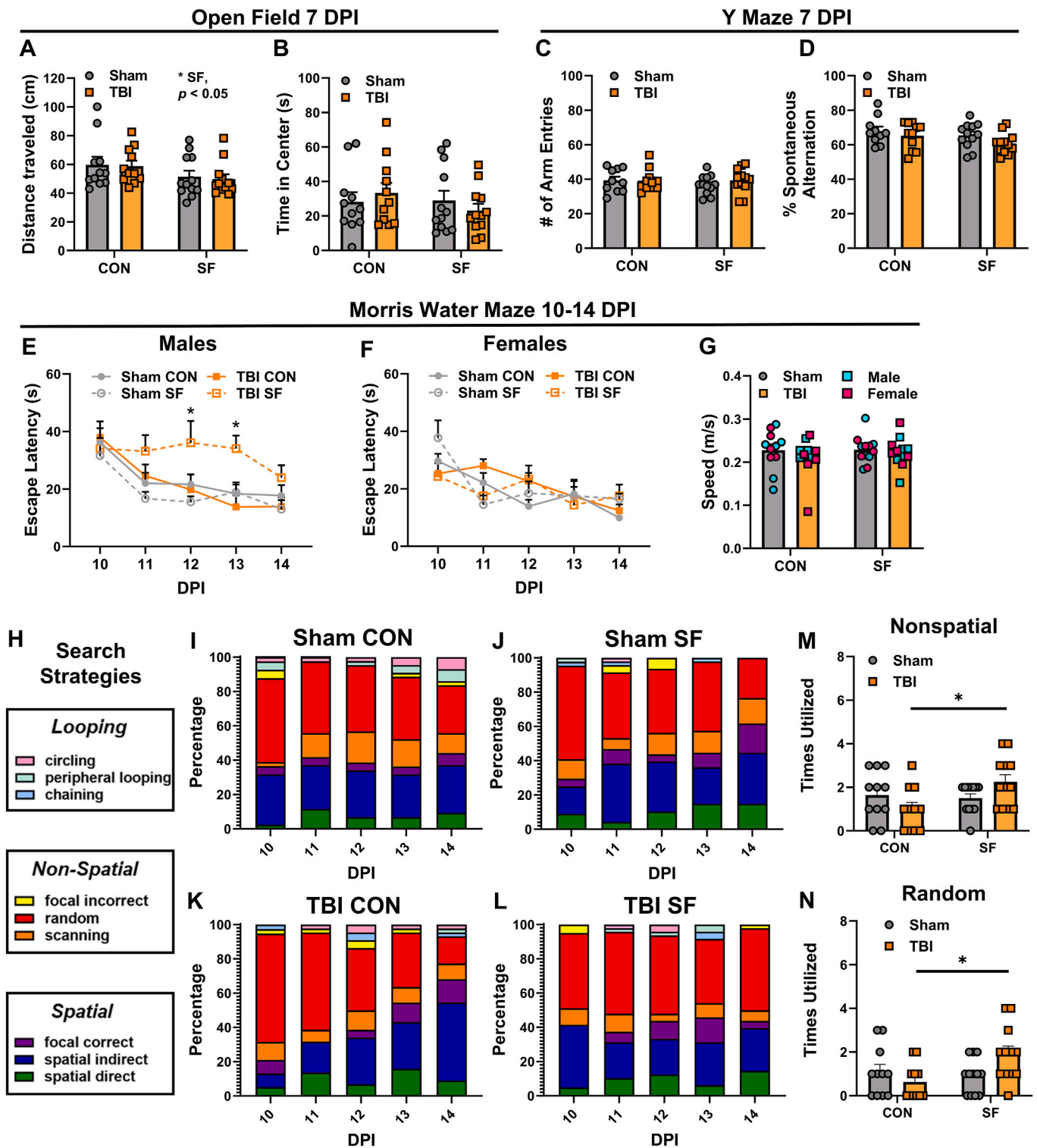
**Fig. 3. Post-Injury SF stress impairs spatial learning and memory 14 DPI.** Anxiety-like behavior was tested 7 DPI in the open field test. (A) SF decreased distance traveled in the open field (SF, p < 0.05, but no differences are observed in time spent in the center of the open field (B). Spatial working memory was tested 7 DPI in the Y maze. No differences were observed in total number of arm entries (C), or percent spontaneous alternations (D). Spatial learning and memory were assessed from 9 to 14 DPI using the MWM. (E) TBI impaired performance in the MWM and male TBI SF mice had longer escape latencies than male TBI control mice (Injury, *p* < 0.05; Injury x SF, *p* < 0.05). (F) No difference in escape latency were detected in female mice. (G) No differences in swim speed were detected between groups or by sex. (I) Sham control, (J) Sham SF, (K) TBI control, and (L) TBI SF mice swim patterns were tracked and assigned to one of (H) nine spatial search strategies. (M) 14 DPI search strategy usage was quantified and TBI SF mice used more non-spatially directed search strategies than TBI control mice (Injury x SF, *p* < 0.05. (N) This effect was driven by a higher use of random search strategies 14 DPI by TBI SF mice compared to TBI control mice (Injury x SF, *p* < 0.05). (Mean ± SEM).
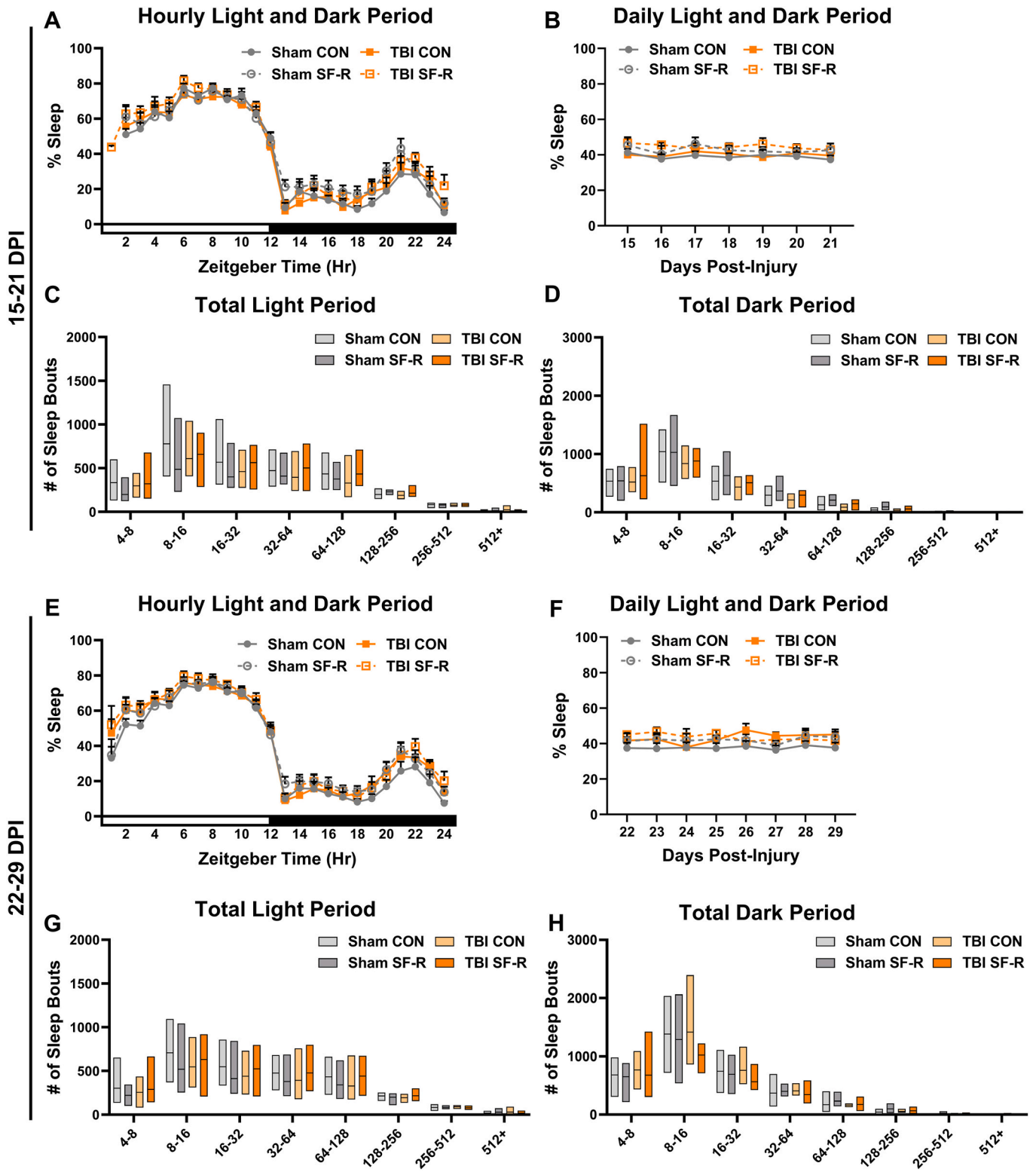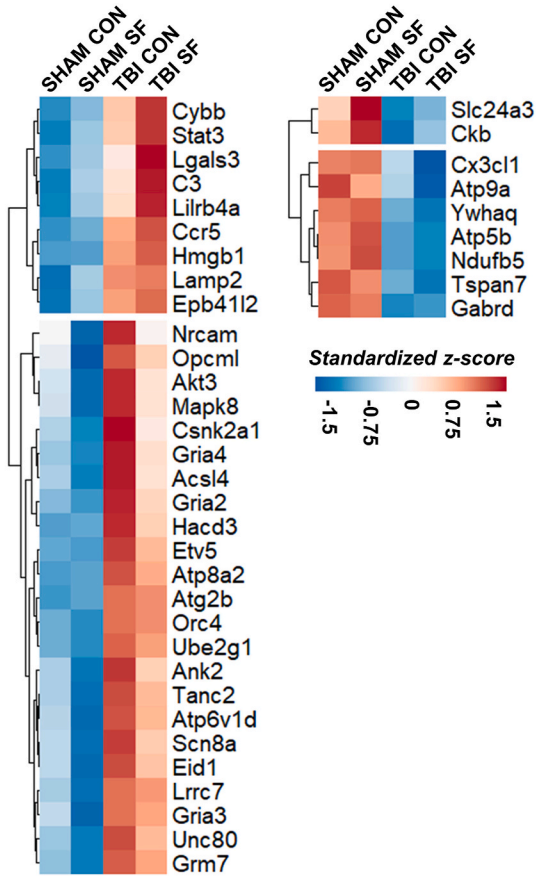
**Fig. 4. SF does not impart lasting deficits in sleep during SF stress recovery period 15–30 DPI.** Percent-sleep and sleep bouts were analyzed for the 16 days following the end of daily mechanical SF at 14 DPI. No differences between groups exist 15–21 DPI when comparing hourly (A) or daily (B) percent-sleep. Sleep bouts from 15 to 21 DPI were separated by light (C) and dark period (D) and no differences between groups are displayed. Analysis for (E) average hourly percent-sleep, (F) daily percent-sleep, (G) light period sleep bouts, (H) and dark period sleep bouts, were repeated for 22–29 DPI and no differences are detected. (Percent-sleep = Mean ± SEM, Sleep bouts = Mean ± max/min).
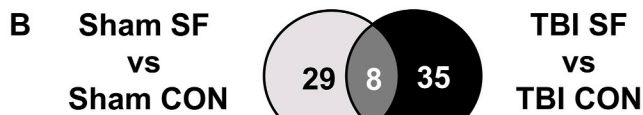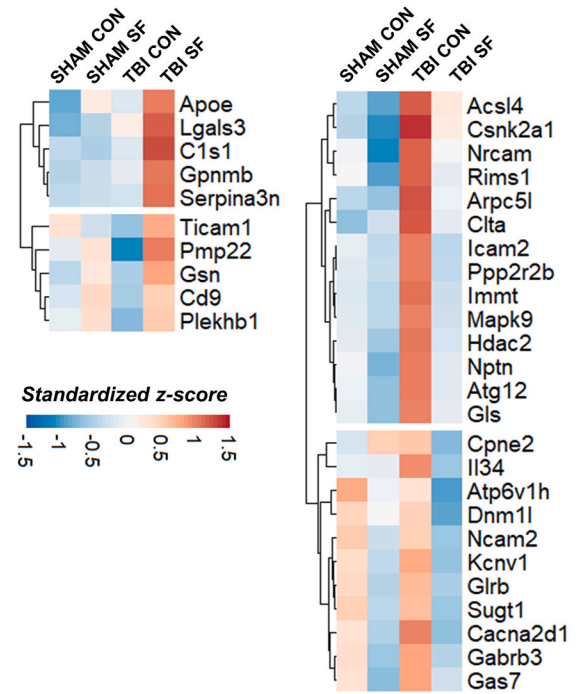
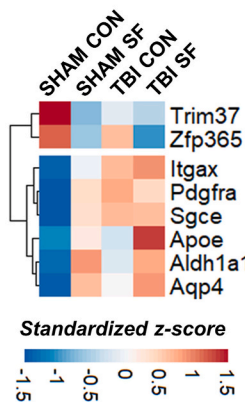**A** TBI CON vs Sham CON — Venn: 91, 41, 97 — TBI SF vs Sham SF
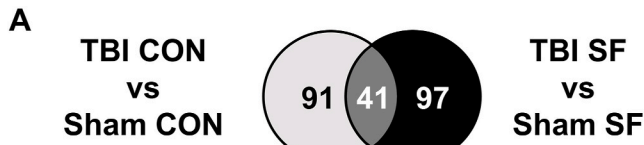
**Overall TBI Effect 14 DPI**

**C** TBI SF vs TBI CON

**D** IPA Upstream Regulators

**B** Sham SF vs Sham CON — Venn: 29, 8, 35 — TBI SF vs TBI CON
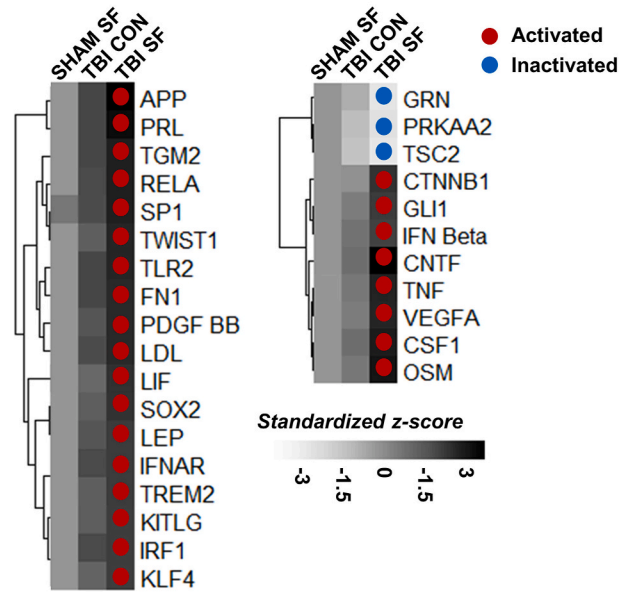
**Overall SF Effect 14 DPI**

*(caption on next page)*

**Fig. 5. Post-TBI SF stress suppresses neurogenesis-related gene expression and increases inflammatory signaling 14 DPI.** (A) Heatmap of the standardized z-scores of significantly changed genes constituting the overall effect of TBI in the ipsilateral cortex 14 DPI. Overall effect of TBI was determined by finding genes that were similarly altered in sham vs TBI comparisons within either the control or SF sleep conditions. (B) Heatmap of the standardized z-scores of significantly changed genes that constitute the overall effect of SF in the ipsilateral cortex 14 DPI. Overall effect of SF was determined by finding genes that were similarly altered in control vs SF comparisons within either sham or TBI conditions. (C) Heatmap of the z-scores of genes increased or decreased in TBI SF mice when compared to TBI control mice. (D) Ingenuity Pathway Analysis (IPA) of top upstream regulators that are either inhibited (Activation z-score $< -2$) or activated (Activation z-score $>2$) uniquely in TBI SF mice when compared to sham control mice. These upstream regulators were not activated or inhibited by any other condition compared to sham control mice. $n = 6$/group.

determined by comparing sham SF to sham control mice and TBI SF to TBI controls and finding the genes that were similarly increased or decreased (Fig. 5B). Eight genes constitute the overall effect of SF stress 14 DPI. Of these, several genes related to astrocyte function were increased including *Apoe*, *Aldh1a1*, and *Aqp4*. Together, these data highlight changes in the transcriptome of the injured cortex following a combination of TBI and SF stress. The DEGs observed support that post-TBI SF stress increases transcription of inflammation related genes and decreases the transcription of neurogenesis related genes.

Next, TBI SF and TBI control groups were compared to find genes that were changed by post-TBI SF (Fig. 5C). Within TBI mice, SF stress increased the expression of genetic markers for primed microglia such as *Apoe*, *Lgals3*, and *Cd9* (Keren-Shaul et al., 2017; Rahimian et al., 2021). Additionally, several neurogenesis-related genes were suppressed such as *Nrcam*, *Ncam2*, and *Nptn* (Ogawa et al., 2023). Many neurogenesis genes that were increased by TBI alone were not increased in TBI SF mice, indicating that post-injury SF stress may impede reparative processes in the post-TBI brain.

These genetic differences within the injured cortex were analyzed using IPA to identify key upstream regulators that were either activated (z-score $>2$) or inhibited (z-score $<2$) in sham SF, TBI control, or TBI SF groups compared to the sham control mice (Fig. 5D). We isolated upstream regulators that were uniquely activated or inhibited by post-TBI SF compared to sham control. Regulators of microglial reactivity IFNβ, TNF, TLR2 and TREM2 were all increased by TBI SF (Babcock et al., 2006; Doğanyiğit et al., 2022; Town et al., 2005; Xue and Du, 2021). Additionally, growth factors such as PDGF, SOX2, and VEGFA were activated specifically by TBI SF. Together these data from 14 DPI show that post-TBI SF stress increased neuroinflammatory signaling while preventing TBI related increases in neurogenesis genes.

### 3.6. TBI SF-R mice show elevated microglia CD68 expression in the hippocampal CA1 30 DPI

We sought to characterize the microglial response to TBI SF after a period of recovery 30 DPI. Groups receiving 14 days of SF are identified as SF-R for the 30 DPI time point. First, we performed IF histochemistry to quantify IBA1 and CD68 expression. Both measures were used to demonstrate changes in microglia activity following TBI and stress (DiSabato et al., 2016; Tapp et al., 2022). We calculated IBA1 percent-area and microglial CD68 expression in the injured lateral cortex as described in the methods (Fig. 6A) as well as in the hippocampal CA1 (Fig. 6D). TBI and SF-R both increased IBA1 percent area in the injured lateral cortex (Injury, $F (1, 18) = 18.72, p < 0.05$; SF, $F (1, 18) = 6.990, p < 0.05$). *Post hoc* analysis showed TBI SF mice expressed higher IBA1 expression than sham control and sham SF-R mice while TBI control mice were not significantly different from any group (Bonferroni, $p < 0.05$; Fig. 6B). SF-R alone increased CD68 expression in the lateral cortex (SF-R, $F (1, 19) = 5.864, p < 0.05$; Fig. 6C).

Next we looked within the hippocampal CA1 (Fig. 6D), a key region in spatial learning and memory, which is also vulnerable to TBI induced inflammation (Muccigrosso et al., 2016; Tapp et al., 2022). We found that TBI and SF-R both increased IBA1 percent-area in the CA1 (Injury, $F (1, 18) = 8.513, p < 0.05$; SF-R, $F (1, 18) = 8.119, p < 0.05$; Fig. 6E). *Post hoc* analysis showed TBI SF mice had higher IBA1 expression than sham control mice (Bonferroni, $p < 0.05$; Fig. 6E). CD68 expression was also elevated by an interaction between TBI and SF (Injury, $F (1, 18) = 8.392,$

$p < 0.05$; TBI x SF-R, $F (1, 19) = 4.548, p < 0.05$; Fig. 6F). *Post hoc* analysis showed that TBI SF-R mice had higher microglial CD68 expression than all other groups (Bonferroni, $p < 0.05$). These data show that 14 days of post-TBI SF can have lasting impacts on microglial function within the brain 30 DPI.

### 3.7. TBI and SF stress do not impact GFAP and CD45 expression near injury site 30 DPI

To assess the potential contribution of reactive astrocytes and leukocytes, we used IF histochemistry to visualize GFAP and CD45 positive cells near the site of injury. GFAP percent-area in the lateral primary somatosensory cortex (Supplementary Fig. 2A) was not significantly different between groups (Supplementary Fig. 2B). CD45 is highly expressed within the CNS in a variety of cells including macrophages, phagocytic microglia, and infiltrating monocytes (Anyaegbu et al., 2021; Dukhinova et al., 2018). which may contribute to the various morphologies present in the injured cortex (Supplementary Fig. 2D). CD45 positive cells within the cortical lesion area were hand counted, and no differences in total number were observed between groups (Supplementary Fig. 2E). These data show that astrocytes and peripheral immune cells are not exaggerating the neuroimmune response in TBI SF-R mice compared to other groups. Nonetheless, additional experiments are needed to clarify the potentially unique role of macrophages and infiltrating monocytes in recovery from post-injury SF stress.

### 3.8. 14 Days of Post-TBI SF stress conveys persistent changes on inflammatory signaling 30 DPI

Next, we evaluated the transcription of inflammation-related genes in the cortex 30 DPI. We determined the overall effects of TBI (Fig. 7A) and SF-R (Fig. 7B), as previously described. 30 DPI TBI increased genes that correspond to microglial driven neuroinflammation including complement factors (*C1qc*, *C1qa*, *C3ar1*, *C4a*, and *C1qb*), phagocytosis marker *CD68*, and homeostatic microglia marker *Ctss* (Nakanishi, 2020). 5 genes related to driving reactive microglia phenotypes were increased including *Clec7a*, *Gpnmb*, *Lgals3*, *Trem2*, and *Tyrobp* (Audrain et al., 2021; Mathys et al., 2017; Satoh et al., 2019). The overall effect of SF stress 30 DPI was limited to one gene *Prkab2* which encodes a regulatory subunit of AMPK.

Next, 14 differentially expressed genes were found between TBI SF-R and TBI control groups. These included increases in key genes involved in microglial reactivity such as *Abca 1*, *Mef2a*, and *Spi1* and decreased *Lpl* expression (Karasinska et al., 2013; Li et al., 2021; Loving et al., 2021; Rustenhoven et al., 2018). *Prkab2* was also increased. Next, we used IPA as previously described to analyze differences in upstream regulators. Many upstream regulators of microglial-driven neuro-inflammation were activated specifically in TBI SF-R mice that were not observed when comparing other groups to the sham controls. These activated upstream regulators included cytokines IL1β, IL33, and IL6, as well as key regulators of cytokine and chemokine production such as NFκB, Vegf, and STAT3. The data show that 14 days of post-TBI SF was sufficient to alter regulation of the inflammatory response 30 DPI.
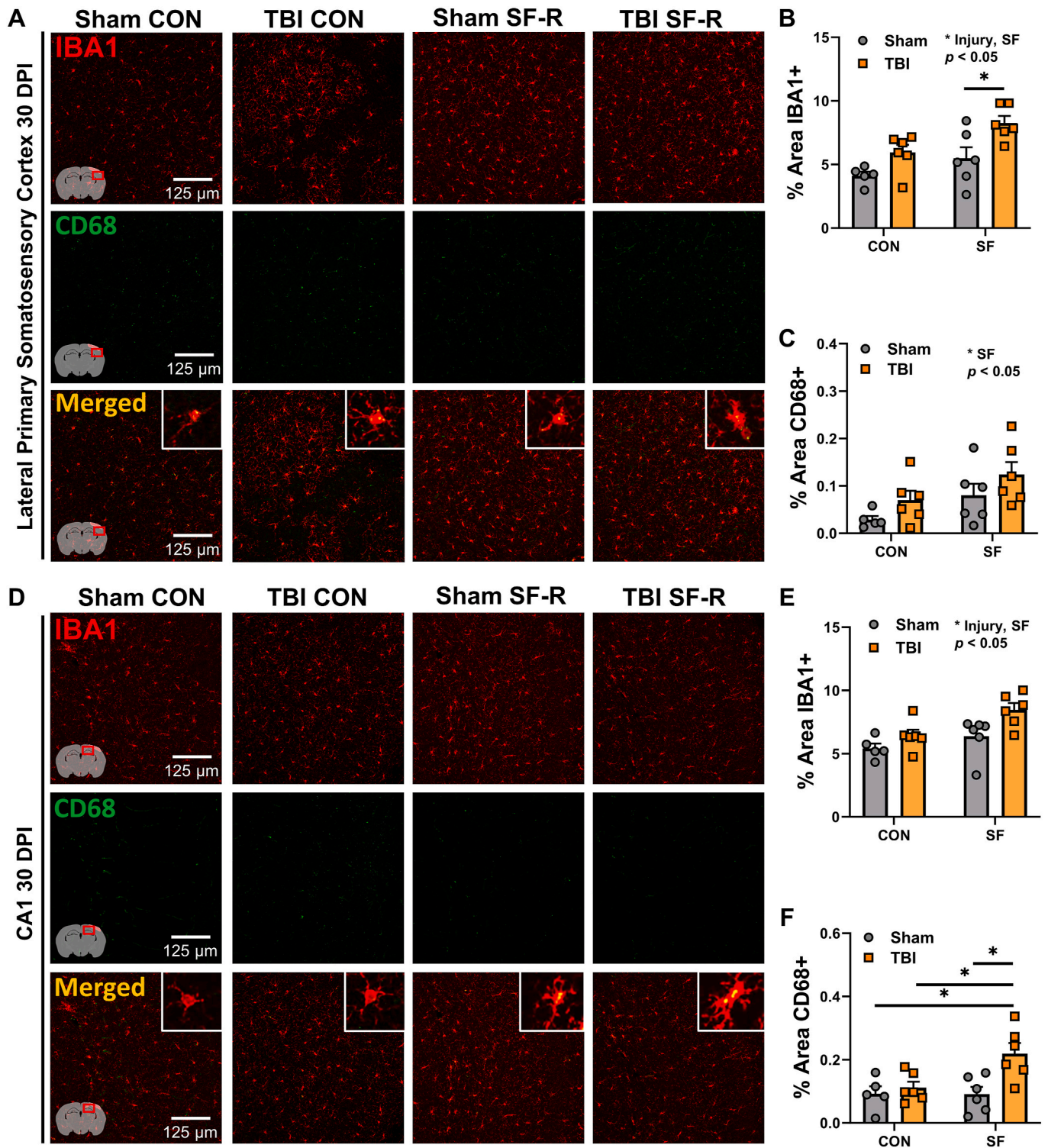
**Fig. 6. Post-TBI SF stress increases IBA1 and CD68 in the ipsilateral cortex and hippocampal CA1 30 DPI.** (A) Representative images of IBA1 and CD68 labeling from the lateral cortex ipsilateral to injury. In the merged images inserts are included to show representative IBA1+/CD68+ microglia. (B) IBA1 percent-area was increased by both TBI and SF (Injury, $p < 0.05$; SF, $p < 0.05$). TBI SF mice had higher IBA1 precent-area than sham SF mice in the lateral cortex ($p < 0.05$). (C) SF increased microglial CD68 percent-area withing the lateral cortex (SF, $p < 0.05$). (D) Representative IBA1 and CD68 images from the hippocampal CA1. (E) TBI and SF (Injury, $p < 0.05$; SF, $p < 0.05$) both increased IBA1 percent-area in the CA1. (F) TBI interacted with SF (Injury, $p < 0.05$; TBI x SF-R, $p < 0.05$). to increase microglial CD68 percent-area in the CA1 where TBI SF mice had higher microglial CD68 percent-area than all other groups.

### 3.9. Post-TBI SF stress impairs and delays the activation of reparative pathways

Finally, we compared activated canonical pathways in brain injured mice 14 and 30 DPI using IPA. First, TBI control mice were compared to sham control mice 14 and 30 DPI. Second, TBI SF-R mice were compared to sham control mice 14 and 30 DPI. Finally, a comparison analysis of the altered relative canonical pathways was completed between TBI and
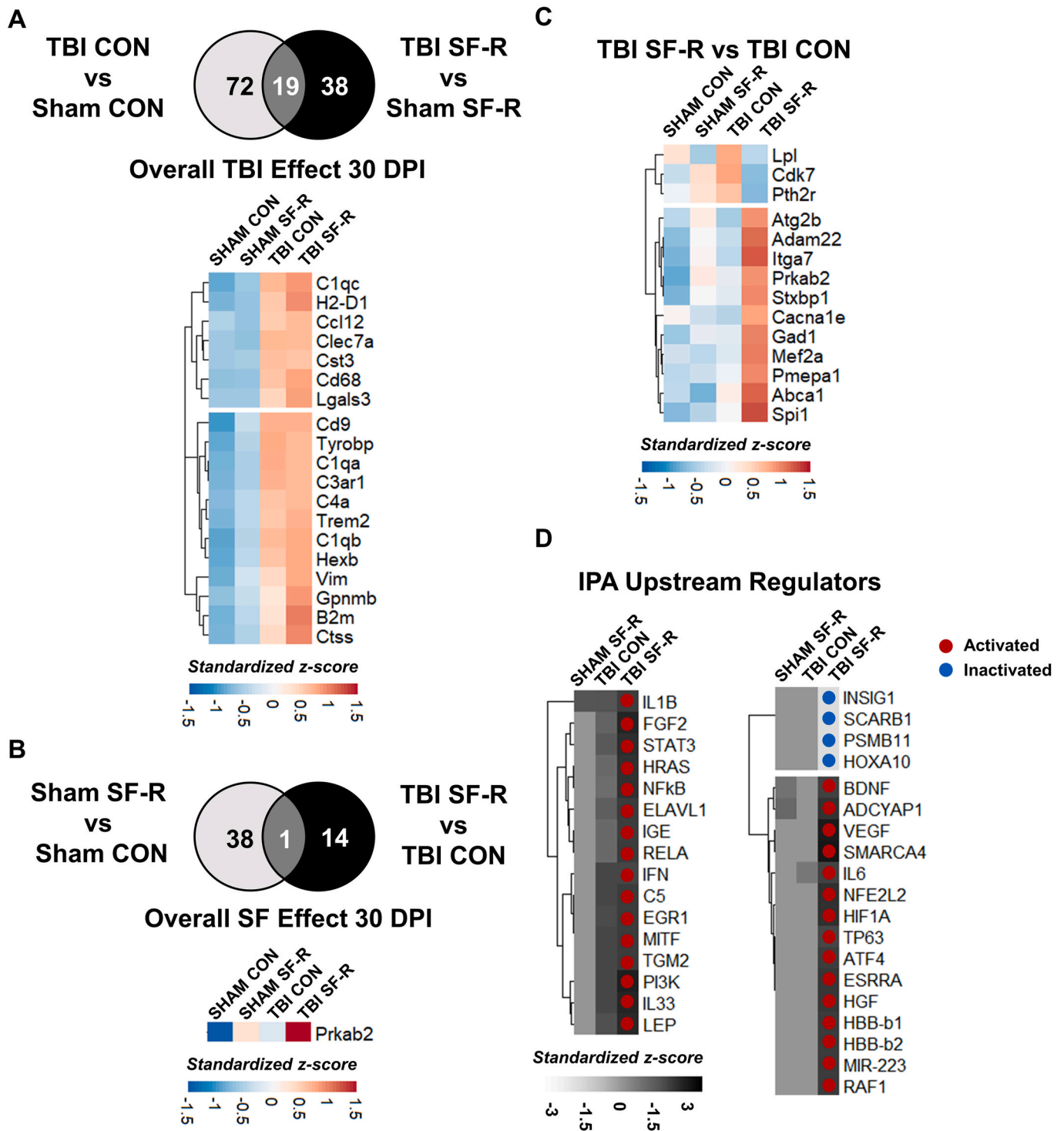
**Fig. 7. Post-TBI SF stress conveys lasting changes on inflammatory signaling 30 DPI.** (A) Heatmap of the standardized z-scores of differentially expressed genes constituting the overall effect of TBI in the ipsilateral cortex 30 DPI. (B) Heatmap of the standardized z-scores of *Prkab2*, the only differentially expressed genes constituting the overall effect of SF in the ipsilateral cortex 30 DPI. (C) Heatmap of the z-scores of genes significantly increased or decreased in TBI SF mice when compared to TBI control mice 30 DPI. (D) Ingenuity Pathway Analysis (IPA) of top upstream regulators that are either inhibited (Activation z-score < −2) or activated (Activation z-score >2) uniquely in TBI SF mice when compared to sham control mice. These upstream regulators were not activated or inhibited by any other condition compared to sham control mice. $n = 6$/group.

TBI SF-R mice 14 and 30 DPI. 14 DPI, TBI control activated several pathways that were not activated in TBI SF mice including the Synaptic LTP, IL-8 signaling, Production of NO and ROS in Macrophages, Apelin Endothelial signaling, and Synaptogenesis signaling pathways (Fig. 8A). The Neuroinflammation signaling pathway, however, was uniquely

activated by post-TBI SF. By 30 DPI we saw similar pathways were affected, however, they were uniquely activated by different conditions (Fig. 8B). At 30 DPI IL-8 signaling, NOS and ROS production, Apelin Endothelial signaling was uniquely activated by post-TBI SF. Additionally, Complement signaling was uniquely activated by post-TBI SF.
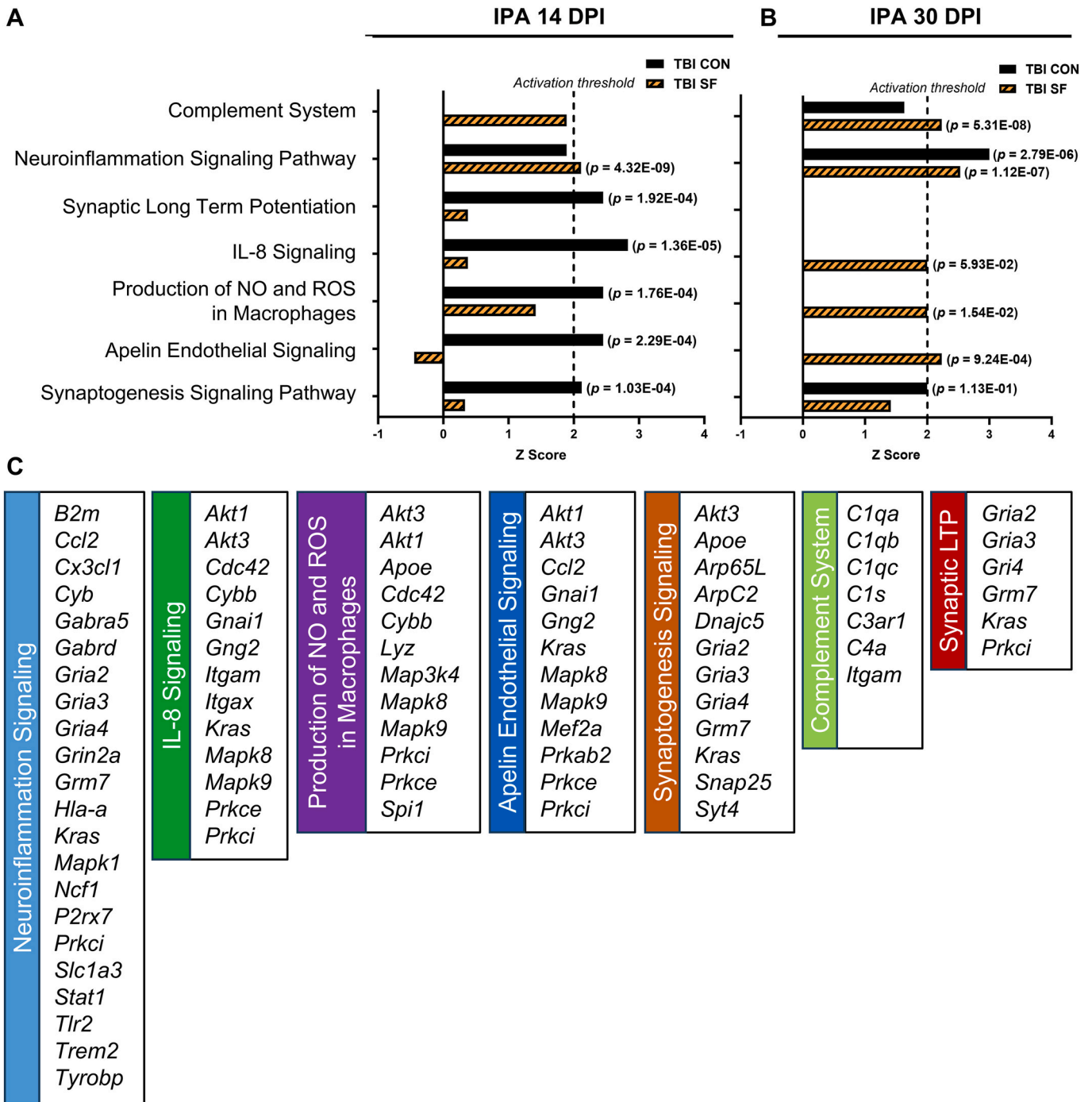
**Fig. 8. Post-TBI SF stress impairs and delays the activation of reparative pathways.** All pathway enrichment was performed using IPA comparison analysis. (A) IPA comparison analysis showing pathways enriched in TBI control mice and TBI SF mice 14 DPI. (B) IPA comparison analysis showing pathways enriched in TBI control and TBI SF mice 30 DPI. (C) DEGs considered within each pathway to determine pathway enrichment.

Synaptogenesis signaling was the sole pathway that was uniquely activated by TBI alone 30 DPI. In full, 58 unique DEGs were included in the analysis of these 7 pathways. DEGs were separated regardless of which timepoint they were compared to identify the number of genes that were considered for each pathway (Fig. 8C). Together, these data show that SF stress after TBI may delay the activation of key reparative pathways.

## 4. Discussion

Here, we sought to evaluate a model of post-TBI SF stress and determine whether 14 days of SF stress would convey subacute and chronic changes in TBI pathophysiology 30 DPI. We hypothesized that SF stress would exaggerate TBI-induced deficits in sleep and behavior and amplify the microglial response to injury, which would persist even after a period of recovery from SF stress. Briefly, we found that the effects of daily SF concentrate during the dark period, increasing sleep during a time when mice are typically most active 1–14 DPI. We also found that mouse sleep normalizes once SF ends 15–30 DPI. SF stress interacted with TBI to impair MWM performance in male mice and affected the adoption of new search strategies in all mice. At 14 DPI we found that genes related to reactive microglia were increased in TBI SF mice while pathway enrichment showed that LTP and synaptogenesis

pathways were activated in TBI control mice but not in TBI SF mice. 30 DPI, the inflammatory transcriptome showed that several genes involved in regulating reactive microglia and several inflammatory upstream regulators remained increased despite a period of recovery from SF stress. 30 DPI, the synaptic pathways previously activated in TBI control mice were now activated in TBI SF-R mice along with unique activation of the Neuroinflammatory pathway 30 DPI. IF from 30 DPI showed that TBI and SF-R increased IBA1 percent-area in the ipsilateral primary somatosensory cortex and in the hippocampal CA1. Additionally, TBI SF-R mice had the highest expression of microglial CD68 in the CA1. In short, these findings support that SF stress exacerbates the inflammatory response to TBI and that this exacerbated inflammatory response can persist despite resolution of post-TBI SF.

These main findings offer several points of discussion. To begin, contrary to our hypothesis, the effects of moderate LFPI alone on sleep were slight and resolved by 7 DPI. These results are in line with previous findings in midline fluid percussion injury models which detailed acute sleep disturbances after TBI that did not persist chronically (Rowe et al., 2014a, 2014b). Dark period percent-sleep increased in SF mice 8–14 DPI, showing that it takes a week of daily SF exposure to affect percent sleep and sleep bout counts in mice. As the dark period corresponds with the active period for mice, these results are analogous to excessive day-time sleepiness which is a commonly reported side effect of SF in human clinical populations (Slater and Steier, 2012).

SF increased the number of 16–64 s sleep bouts, while TBI decreased the number of 256–512 s sleep bouts 1–7 DPI. Therefore, TBI impairs sleep consolidation thereby decreasing overall percent sleep 1–7 DPI. 8–14 DPI, sham SF mice engaged in more sleep bouts than sham control mice. Similar increases were not seen in the TBI SF mice suggesting that TBI may impair the ability of mice to adequately adapt their sleep to account for environmental SF. The use of piezoelectric sleep monitoring systems for this study provided several advantages and limitations. These sleep systems offer a noninvasive alternative to EEG for the purposes of tracking the quantity of mouse sleep and the length of sleep bouts. This was an important consideration in this study as EEG implant surgery would serve as an additional source of secondary neuroinflammation that could confound the ability to examine the relationship between TBI and SF-induced stress response. One limitation of these systems is their inability to discern sleep stages such as non-rapid eye movement (NREM) or REM sleep. Also, we had to eliminate 5 h of sleep-wake analysis during the SF period. Therefore, additional studies are needed to determine if and how post-TBI SF influences NREM and REM sleep during SF stress exposure and in response to SF stress. It is notable that detectable alterations in sleep resolved immediately upon removal of daily SF. The lack of persistent deficits in sleep during SF-R demonstrates that any observed changes in inflammatory gene transcription or microglial phenotypes in TBI SF mice are due to the previous exposure to SF stress.

Following TBI, we tested spatial working memory in the Y maze 7 DPI, and spatial learning and reference memory in the MWM 9–14 DPI. No differences were seen between groups in the Y maze; however, male TBI SF mice had deficits in latency to escape the MWM. These results support the idea that 7 days of SF stress was not sufficient to interact with TBI and induce deficits in cognition. SF stress interacts with TBI in male animals to increase the latency to escape the MWM 12 and 13 DPI; however, both male and female TBI SF mice disproportionally used random search strategies. Previous studies have shown that SF specifically affects spatial reference memory but not spatial working memory (Ward et al., 2009). Therefore, the MWM may be particularly well suited to study the interaction effect between SF stress and TBI.

The sex-specific effect of post-TBI SF on MWM performance is of particular interest. These findings are in line with previous work showing that moderate LFPI produces sex-specific deficits in anterograde memory (Fitzgerald et al., 2022). Therefore, in our post-TBI stress model, the male mouse brain may be vulnerable to memory impairment. SF stress may then provide the "tipping point" in male mice and drive

post-TBI cognitive deficits not observed in female mice. Additionally, while this sex effect was observed when measuring latency to escape the MWM, no effect of sex was observed when analyzing the changes in search strategy. Males and females were equally impaired. Sex effects were not found anywhere else in these studies. However, it is worth noting that additional studies are required to better understand sex specific differences.

Several points for discussion arise when analyzing DEGs from the whole injured cortex at 14 and 30 DPI. Only one DEG, *Prkab2*, was increased by SF 14 DPI. *Prkab2* encodes a regulatory subunit of AMPK which is a mediating factor in cellular and mitochondrial stress. AMPK/ CREB signaling has been shown to be active following TBI and is a potential therapeutic target to improve outcomes (Hill et al., 2016; Wu and Zou, 2020). Additionally, *Prkab2* is specifically linked to the homeostatic regulation of rebound sleep following periods of sleep deprivation (Pinto et al., 2023). Therefore, increases in *Prkab2* gene expression may be a factor in regulating the return to typical sleep following the prior removal of SF 14 DPI. Additionally, post-TBI SF decreased expression of cortical genes involved with neurogenesis such as *Ncam2* and *Nptn* 14 DPI. These initial results suggested that post-TBI SF may be impairing pro-recovery pathways stimulating neurogenesis that would normally aid in TBI recovery. To see whether this impairment persisted after SF ended, we used the same glial profiling panels on RNA from the injured cortex 30 DPI. We did observe increases in genes associated with heightened neuroinflammation in TBI SF-R mice 30 DPI, including increased *Mef2a* and *Spi1*. However, the lack of changes in genes that were clear markers for neurogenesis were noticeable. Therefore, we used IPA canonical pathway analysis to determine differences in pathway enrichment between 14 and 30 DPI.

We found the Neuroinflammation pathway was activated in TBI SF but not TBI control animals 14 DPI. Additionally, Synaptic LTP, and Synaptogenesis Signaling pathways were activated in TBI control mice but not TBI SF mice. Together, these differentially activated pathways suggest that cortical neuroinflammation is increased while critical post-TBI reparative pathways related to neuronal function are suppressed in TBI mice after 14 days of SF. Suppression of synaptic LTP by TBI SF corresponds with our findings from the MWM where spatial learning and memory was impaired in male TBI SF mice. While gene expression within the hippocampus was not explored here, follow up studies could be useful for determining whether similar processes are impaired in the hippocampus.

Similar trends in pathway enrichment emerged 30 DPI. Canonical pathway analysis revealed that several pathways that were selectively activated in TBI control mice 14 DPI were then activated in TBI SF-R conditions 30 DPI. One possible explanation is that components of these pathways may be involved in early tissue repair following brain injury and are initially suppressed by ongoing SF stress 14 DPI. Then, removal of daily SF allows for delayed activation of some of these repair pathways. These pathways included IL-8 Signaling, Production of NO and ROS in Macrophages, and Apelin Endothelial Signaling. IL-8 in humans is involved in the chemoattraction of cells like neutrophils soon after TBI (Woodcock and Morganti-Kossmann, 2013). Apelin signaling is involved during the early phases of TBI support endothelial cells and maintain blood brain barrier (BBB) integrity (Xu et al., 2019). These results are in accordance with our previous findings that TBI SF-R dysregulated aquaporin-4 polarization indicating that BBB integrity was compromised by TBI SF-R. Together these data suggest that SF impairs or delays recovery processes following TBI.

Most DEGs considered by IPA were derived from the Neuroinflammation Signaling Pathway which was selectively activated by TBI SF at 14 DPI and by both TBI CON and TBI SF-R at 30 DPI. Amongst these DEGs many genes found were involved in the regulation of microglial reactivity including: *Ccl2*, *Cx3cr1*, *P2rx7*, *Tlr2/7*, and *Trem2*. Even in synaptic function-related pathways such as the Synaptogenesis Signaling pathway several DEGs were considered that are typically highly enriched in microglia such as: *Apoe*, *Arpc5l*, and *Kras* (Zhang

et al., 2014). Enrichment of the Complement System may provide further evidence of a microglial role in synaptogenesis following TBI SF-R. Complement is heavily used by microglia to target synapses for pruning during synaptogenesis and has been hypothesized to be a potential mechanism of secondary injury following TBI (Gomez-Arboledas et al., 2021).

Microglia play key roles in synaptogenesis and synaptic remodeling following TBI. Post-TBI SF may influence these processes by microglial-specific mechanisms which warrant further consideration (Krukowski et al., 2021). Indeed, when looking at markers for microglial reactivity and phagocytosis 30 DPI we found elevated microglial CD68 expression in the hippocampal CA1. Further work needs to be done to examine the role of microglia in synaptic remodeling under TBI SF conditions, and whether this chronic, heightened neuroinflammation could continue to impair functional recovery from TBI. All together these findings show that exposure to even a few weeks of post-TBI SF imparts cognitive deficits, heightens inflammatory gene expression and microglial activity, and suppresses synaptogenesis signaling pathways.

There are some study limitations that should be considered when interpreting the results. For example, single-housing mice has been shown to be psychologically stressful (Manouze et al., 2019). The adapt-a-base system used for sleep monitoring requires only one mouse be present in the recording cage at a time. Therefore, singly-housed mice were used for sleep and RNA outcome measures, and group housed mice were used for behavioral studies and IF. It is also important to underscore that changes at the RNA level do not necessarily dictate changes at the protein level. Thus, changes in the counts of individual transcripts should be viewed as suggestive of pathways that may be affected by TBI and SF stress. Finally, RNA was obtained by digestion of the whole injured cortex, and an exclusive list of antibodies was used for IF histochemistry. TBI alone increased IBA1 percent-area in the ipsilateral primary somatosensory cortex, which is consistent with our previous 60 DPI study (Tapp et al., 2023). However, TBI did not result in elevated cortical GFAP expression, and TBI SF-R did not exaggerate the number of cortical CD45 positive cells 30 DPI. We hypothesize that there is a delayed effect of SF stress that engages astrocytes and peripheral immune cells over time; however, additional studies are needed to clarify the role of specific cell populations, including microglia, astrocytes, and peripheral immune cells.

## 5. Conclusions

In conclusion, post-TBI SF stress had several acute and long-term effects that merit consideration in future studies. The ability of post-TBI SF stress to impair spatial memory performance and delay the activation of synapse-related pathways in the cortex are particularly consequential for this field of study moving forward. These data show that transient SF stress after TBI impairs recovery and conveys long-lasting impacts on neuroimmune function independent of continuous sleep deficits. Together, these findings support that even limited exposure to post-TBI stress can have lasting impacts on cognitive recovery and regulation of the immune response to trauma.

## Author disclosure

Nothing to Report.

## Funding statement

## CRediT authorship contribution statement

**Samuel Houle:** Conceptualization, Formal analysis, Investigation, Methodology, Software, Visualization, Writing – original draft. **Zoe Tapp:** Methodology, Visualization, Writing – original draft. **Shannon Dobres:** Formal analysis, Visualization, Writing – original draft. **Sakeef Ahsan:** Formal analysis, Investigation, Visualization, Writing – original draft. **Yvanna Reyes:** Formal analysis, Investigation, Visualization, Writing – review & editing. **Christopher Cotter:** Investigation, Writing – review & editing. **Jessica Mitsch:** Formal analysis, Investigation, Visualization, Writing – review & editing. **Zachary Zimomra:** Investigation, Project administration, Resources, Writing – review & editing. **Juan Peng:** Formal analysis, Software, Writing – original draft. **Rachel K. Rowe:** Formal analysis, Methodology, Writing – review & editing. **Jonathan Lifshitz:** Formal analysis, Methodology, Writing – review & editing. **John Sheridan:** Conceptualization, Resources, Supervision, Writing – review & editing. **Jonathan Godbout:** Conceptualization, Resources, Supervision, Writing – review & editing. **Olga N. Kokiko-Cochran:** Conceptualization, Formal analysis, Funding acquisition, Methodology, Project administration, Resources, Supervision, Writing – original draft.

## Declaration of competing interest

None.

## Acknowledgements

## Appendix A. Supplementary data

Supplementary data to this article can be found online at https://doi.org/10.1016/j.bbih.2024.100797.

## References

Ahmed, S., Venigalla, H., Mekala, H.M., Dar, S., Hassan, M., Ayub, S., 2017. Traumatic brain injury and neuropsychiatric complications. Indian J. Psychol. Med. https://doi.org/10.4103/0253-7176.203129.

Anyaegbu, C.C., Mao, Y., McGonigle, T., Raja, S., Clarke, T., Solomon, T., Black, A.M.B., Fuller, K., Fitzgerald, M., 2021. Simultaneous flow cytometric characterization of multiple cell types and metabolic states in the rat brain after repeated mild traumatic brain injury. J. Neurosci. Methods 359, 109223. https://doi.org/10.1016/j.jneumeth.2021.109223.

Audrain, M., Haure-Mirande, J., Mleczko, J., Wang, M., Griffin, J.K., St George-Hyslop, P. H., Fraser, P., Zhang, B., Gandy, S., Ehrlich, M.E., 2021. Reactive or transgenic increase in microglial TYROBP reveals a TREM2-independent TYROBP–APOE link in wild-type and Alzheimer's-related mice. Alzheimer's Dementia 17, 149–163. https://doi.org/10.1002/alz.12256.

Babcock, A.A., Wirenfeldt, M., Holm, T., Nielsen, H.H., Dissing-Olesen, L., Toft-Hansen, H., Millward, J.M., Landmann, R., Rivest, S., Finsen, B., Owens, T., 2006. Toll-like receptor 2 signaling in response to brain injury: an innate bridge to neuroinflammation. J. Neurosci. 26, 12826–12837. https://doi.org/10.1523/JNEUROSCI.4937-05.2006.

Bray, C.E., Witcher, K.G., Adekunle-Adegbite, D., Ouvina, M., Witzel, M., Hans, E., Tapp, Z.M., Packer, J., Goodman, E., Zhao, F., Chunchai, T., O'Neil, S., Chattipakorn, S.C., Sheridan, J., Kokiko-Cochran, O.N., Askwith, C., Godbout, J.P., 2022. Chronic cortical inflammation, cognitive impairment, and immune reactivity associated with diffuse brain injury are ameliorated by forced turnover of microglia. J. Neurosci. 42, 4215–4228. https://doi.org/10.1523/JNEUROSCI.1910-21.2022.

Brody, D.L., Holtzman, D.M., 2006. Morris water maze search strategy analysis in PDAPP mice before and after experimental traumatic brain injury. Exp. Neurol. 197, 330–340. https://doi.org/10.1016/j.expneurol.2005.10.020.

Chan, L.G., Feinstein, A., 2015. Persistent sleep disturbances independently predict poorer functional and social outcomes 1 Year after mild traumatic brain injury. J. Head Trauma Rehabil. 30, E67–E75. https://doi.org/10.1097/HTR.0000000000000119.

Chen, J., Buchanan, J.B., Sparkman, N.L., Godbout, J.P., Freund, G.G., Johnson, R.W., 2008. Neuroinflammation and disruption in working memory in aged mice after acute stimulation of the peripheral innate immune system. Brain Behav. Immun. 22, 301–311. https://doi.org/10.1016/j.bbi.2007.08.014.

Cunningham, C., Wilcockson, D.C., Campion, S., Lunnon, K., Perry, V.H., 2005. Central and systemic endotoxin challenges exacerbate the local inflammatory response and increase neuronal death during chronic neurodegeneration. J. Neurosci. 25, 9275–9284. https://doi.org/10.1523/JNEUROSCI.2614-05.2005.

DiSabato, D.J., Quan, N., Godbout, J.P., 2016. Neuroinflammation: the devil is in the details. J. Neurochem. 139, 136–153. https://doi.org/10.1111/JNC.13607.

Doğanyiğit, Z., Erbakan, K., Akyuz, E., Polat, A.K., Arulsamy, A., Shaikh, M.F., 2022. The role of neuroinflammatory mediators in the pathogenesis of traumatic brain injury: a narrative review. ACS Chem. Neurosci. 13, 1835–1848. https://doi.org/10.1021/acschemneuro.2c00196.

Donohue, K.D., Medonza, D.C., Crane, E.R., O'Hara, B.F., 2008. Assessment of a non-invasive high-throughput classifier for behaviours associated with sleep and wake in mice. Biomed. Eng. Online 7, 14. https://doi.org/10.1186/1475-925X-7-14.

Drake, C.L., Cheng, P., Almeida, D.M., Roth, T., 2017. Familial risk for insomnia is associated with abnormal cortisol response to stress. Sleep 40. https://doi.org/10.1093/sleep/zsx143.

Dukhinova, M., Kopeikina, E., Ponomarev, E.D., 2018. Usage of multiparameter flow cytometry to study microglia and macrophage heterogeneity in the central nervous system during neuroinflammation and neurodegeneration, 167–177. https://doi.org/10.1007/978-1-4939-7680-5_10.

Faul, M., Coronado, V., 2015. Epidemiology of traumatic brain injury. In: Handbook of Clinical Neurology. Elsevier B.V., pp. 3–13. https://doi.org/10.1016/B978-0-444-52892-6.00001-5

Fenn, A.M., Gensel, J.C., Huang, Y., Popovich, P.G., Lifshitz, J., Godbout, J.P., 2014. Immune activation promotes depression 1 month after diffuse brain injury: a role for primed microglia. Biol. Psychiatr. 76, 575–584. https://doi.org/10.1016/j.biopsych.2013.10.014.

Fitzgerald, J., Houle, S., Cotter, C., Zimomra, Z., Martens, K.M., Vonder Haar, C., Kokiko-Cochran, O.N., 2022. Lateral fluid percussion injury causes sex-specific deficits in anterograde but not retrograde memory. Front. Behav. Neurosci. 16 https://doi.org/10.3389/FNBEH.2022.806598.

Frank, M.G., Thompson, B.M., Watkins, L.R., Maier, S.F., 2012. Glucocorticoids mediate stress-induced priming of microglial pro-inflammatory responses. Brain Behav. Immun. 26, 337–345. https://doi.org/10.1016/j.bbi.2011.10.005.

Gomez-Arboledas, A., Acharya, M.M., Tenner, A.J., 2021. The role of complement in synaptic pruning and neurodegeneration. ImmunoTargets Ther. 10, 373–386. https://doi.org/10.2147/ITT.S305420.

Goyal, K., Yadav, R., 2020. Traumatic brain injury. In: Acute Neuro Care: Focused Approach to Neuroemergencies. Springer, Singapore, pp. 139–158. https://doi.org/10.1007/978-981-15-4071-4_8.

Henry, C.J., Huang, Y., Wynne, A.M., Godbout, J.P., 2009. Peripheral lipopolysaccharide (LPS) challenge promotes microglial hyperactivity in aged mice that is associated with exaggerated induction of both pro-inflammatory IL-1β and anti-inflammatory IL-10 cytokines. Brain Behav. Immun. 23, 309–317. https://doi.org/10.1016/j.bbi.2008.09.002.

Hill, J.L., Kobori, N., Zhao, J., Rozas, N.S., Hylin, M.J., Moore, A.N., Dash, P.K., 2016. Traumatic brain injury decreases AMP-activated protein kinase activity and pharmacological enhancement of its activity improves cognitive outcome. J. Neurochem. 139, 106–119. https://doi.org/10.1111/jnc.13726.

Hinwood, M., Morandini, J., Day, T.A., Walker, F.R., 2012. Evidence that microglia mediate the neurobiological effects of chronic psychological stress on the medial prefrontal cortex. Cerebr. Cortex 22, 1442–1454. https://doi.org/10.1093/cercor/bhr229.

Hirotsu, C., Tufik, S., Andersen, M.L., 2015. Interactions between sleep, stress, and metabolism: from physiological to pathological conditions. Sleep Sci 8, 143–152. https://doi.org/10.1016/j.slsci.2015.09.002.

Houle, S., Kokiko-Cochran, O.N., 2022. A levee to the flood: pre-injury neuroinflammation and immune stress influence traumatic brain injury outcome. Front. Aging Neurosci. 13 https://doi.org/10.3389/fnagi.2021.788055.

Izzy, S., Liu, Q., Fang, Z., Lule, S., Wu, L., Chung, J.Y., Sarro-Schwartz, A., Brown-Whalen, A., Perner, C., Hickman, S.E., Kaplan, D.L., Patsopoulos, N.A., El Khoury, J., Whalen, M.J., 2019. Time-dependent changes in microglia transcriptional networks following traumatic brain injury. Front. Cell. Neurosci. 13 https://doi.org/10.3389/fncel.2019.00307.

Johnson, V.E., Stewart, J.E., Begbie, F.D., Trojanowski, J.Q., Smith, D.H., Stewart, W., 2013. Inflammation and white matter degeneration persist for years after a single traumatic brain injury. Brain 136, 28–42. https://doi.org/10.1093/brain/aws322.

Kalmbach, D.A., Anderson, J.R., Drake, C.L., 2018a. The impact of stress on sleep: pathogenic sleep reactivity as a vulnerability to insomnia and circadian disorders. J. Sleep Res. 27 https://doi.org/10.1111/jsr.12710.

Kalmbach, D.A., Conroy, D.A., Falk, H., Rao, V., Roy, D., Peters, M.E., Van Meter, T.E., Korley, F.K., 2018b. Poor sleep is linked to impeded recovery from traumatic brain injury. Sleep 41. https://doi.org/10.1093/sleep/zsy147.

Karasinska, J.M., de Haan, W., Franciosi, S., Ruddle, P., Fan, J., Kruit, J.K., Stukas, S., Lütjohann, D., Gutmann, D.H., Wellington, C.L., Hayden, M.R., 2013. ABCA1 influences neuroinflammation and neuronal death. Neurobiol. Dis. 54, 445–455. https://doi.org/10.1016/j.nbd.2013.01.018.

Keren-Shaul, H., Spinrad, A., Weiner, A., Matcovitch-Natan, O., Dvir-Szternfeld, R., Ulland, T.K., David, E., Baruch, K., Lara-Astaiso, D., Toth, B., Itzkovitz, S., Colonna, M., Schwartz, M., Amit, I., 2017. A unique microglia type associated with restricting development of Alzheimer's disease. Cell 169, 1276–1290.e17. https://doi.org/10.1016/J.CELL.2017.05.018.

Kokiko-Cochran, O.N., Godbout, J.P., 2018. The inflammatory continuum of traumatic brain injury and Alzheimer's disease. Front. Immunol. https://doi.org/10.3389/fimmu.2018.00672.

Kokiko-Cochran, O.N., Saber, M., Puntambekar, S., Bemiller, S.M., Katsumoto, A., Lee, Y.-S., Bhaskar, K., Ransohoff, R.M., Lamb, B.T., 2018. Traumatic brain injury in hTau model mice: enhanced acute macrophage response and altered long-term recovery. https://doi.org/10.1089/NEU.2017.5203.

Krukowski, K., Nolan, A., Becker, M., Picard, K., Vernoux, N., Frias, E.S., Feng, X., Tremblay, M.-E., Rosi, S., 2021. Novel microglia-mediated mechanisms underlying synaptic loss and cognitive impairment after traumatic brain injury. Brain Behav. Immun. 98, 122–135. https://doi.org/10.1016/j.bbi.2021.08.210.

Laskowski, R.A., Creed, J.A., Raghupathi, R., 2015. Pathophysiology of mild TBI: implications for altered signaling pathways. In: Brain Neurotrauma: Molecular, Neuropsychological, and Rehabilitation Aspects. CRC Press, pp. 35–42. https://doi.org/10.1201/b18126.

Li, H., Wang, F., Guo, X., Jiang, Y., 2021. Decreased MEF2A expression regulated by its enhancer methylation inhibits autophagy and may play an important role in the progression of Alzheimer's disease. Front. Neurosci. 15 https://doi.org/10.3389/fnins.2021.682247.

Loving, B.A., Tang, M., Neal, M.C., Gorkhali, S., Murphy, R., Eckel, R.H., Bruce, K.D., 2021. Lipoprotein lipase regulates microglial lipid droplet accumulation. Cells 10, 198. https://doi.org/10.3390/cells10020198.

Manouze, H., Ghestem, A., Poillerat, V., Bennis, M., Ba-M'hamed, S., Benoliel, J.J., Becker, C., Bernard, C., 2019. Effects of single cage housing on stress, cognitive, and seizure parameters in the rat and mouse pilocarpine models of epilepsy. ENEURO.0179-18.2019 eneuro 6. https://doi.org/10.1523/ENEURO.0179-18.2019.

Mathias, J.L., Alvaro, P.K., 2012. Prevalence of sleep disturbances, disorders, and problems following traumatic brain injury: a meta-analysis. Sleep Med. 13, 898–905. https://doi.org/10.1016/j.sleep.2012.04.006.

Mathys, H., Adaikkan, C., Gao, F., Young, J.Z., Manet, E., Hemberg, M., De Jager, P.L., Ransohoff, R.M., Regev, A., Tsai, L.-H., 2017. Temporal tracking of microglia activation in neurodegeneration at single-cell resolution. Cell Rep. 21, 366–380. https://doi.org/10.1016/j.celrep.2017.09.039.

Medic, G., Wille, M., Hemels, M., 2017. Short- and long-term health consequences of sleep disruption. Nat. Sci. Sleep 9, 151–161. https://doi.org/10.2147/NSS.S134864.

Muccigrosso, M.M., Ford, J., Benner, B., Moussa, D., Burnsides, C., Fenn, A.M., Popovich, P.G., Lifshitz, J., Walker, F.R., Eiferman, D.S., Godbout, J.P., 2016. Cognitive deficits develop 1 month after diffuse brain injury and are exaggerated by microglia-associated reactivity to peripheral immune challenge. Brain Behav. Immun. 54, 95–109. https://doi.org/10.1016/j.BBI.2016.01.009.

Nakanishi, H., 2020. Cathepsin regulation on microglial function. Biochim. Biophys. Acta, Proteins Proteomics 1868, 140465. https://doi.org/10.1016/j.bbapap.2020.140465.

Norden, D.M., Godbout, J.P., 2013. Review: microglia of the aged brain: primed to be activated and resistant to regulation. Neuropathol. Appl. Neurobiol. 39, 19–34. https://doi.org/10.1111/j.1365-2990.2012.01306.x.

Ogawa, B., Nakanishi, Y., Wakamatsu, M., Takahashi, Y., Shibutani, M., 2023. Repeated administration of acrylamide for 28 days suppresses adult neurogenesis of the olfactory bulb in young-adult rats. Toxicol. Lett. 378, 1–9. https://doi.org/10.1016/J.TOXLET.2023.02.004.

Peterson, A.L., Goodie, J.L., Satterfield, W.A., Brim, W.L., 2008. Sleep disturbance during military deployment. Mil. Med. 173, 230–235. https://doi.org/10.7205/MILMED.173.3.230.

Pinto, M.J., Cottin, L., Dingli, F., Laigle, V., Ribeiro, L.F., Triller, A., Henderson, F., Loew, D., Fabre, V., Bessis, A., 2023. Microglial TNFα orchestrates protein phosphorylation in the cortex during the sleep period and controls homeostatic sleep. EMBO J. 42 https://doi.org/10.15252/embj.2022111485.

Rahimian, R., Béland, L.C., Sato, S., Kriz, J., 2021. Microglia-derived galectin-3 in neuroinflammation; a bittersweet ligand? Med. Res. Rev. 41, 2582–2589. https://doi.org/10.1002/MED.21784.

Raj, R., Kaprio, J., Jousilahti, P., Korja, M., Siironen, J., 2022. Risk of dementia after hospitalization due to traumatic brain injury. Neurology 98, e2377–e2386. https://doi.org/10.1212/WNL.0000000000200290.

Rowe, R.K., Harrison, J.L., O'Hara, B.F., Lifshitz, J., 2014a. Diffuse brain injury does not affect chronic sleep patterns in the mouse. Brain Inj. 28, 504–510. https://doi.org/10.3109/02699052.2014.888768.

Rowe, R.K., Striz, M., Bachstetter, A.D., Van Eldik, L.J., Donohue, K.D., O'Hara, B.F., Lifshitz, J., 2014b. Diffuse brain injury induces acute post-traumatic sleep. PLoS One 9, e82507. https://doi.org/10.1371/journal.pone.0082507.

Rustenhoven, J., Smith, A.M., Smyth, L.C., Jansson, D., Scotter, E.L., Swanson, M.E.V., Aalderink, M., Coppieters, N., Narayan, P., Handley, R., Overall, C., Park, T.I.H., Schweder, P., Heppner, P., Curtis, M.A., Faull, R.L.M., Dragunow, M., 2018. PU.1 regulates Alzheimer's disease-associated genes in primary human microglia. Mol. Neurodegener. 13, 44. https://doi.org/10.1186/s13024-018-0277-1.

Satoh, J., Kino, Y., Yanaizu, M., Ishida, T., Saito, Y., 2019. Microglia express GPNMB in the brains of Alzheimer's disease and Nasu-Hakola disease. Intractable Rare Dis. Res. 8, 120–128. https://doi.org/10.5582/irdr.2019.01049.

Schindelin, J., Arganda-Carreras, I., Frise, E., Kaynig, V., Longair, M., Pietzsch, T., Preibisch, S., Rueden, C., Saalfeld, S., Schmid, B., Tinevez, J.-Y., White, D.J., Hartenstein, V., Eliceiri, K., Tomancak, P., Cardona, A., 2012. Fiji: an open-source platform for biological-image analysis. Nat. Methods 9, 676–682. https://doi.org/10.1038/nmeth.2019.

Slater, G., Steier, J., 2012. Excessive daytime sleepiness in sleep disorders. J. Thorac. Dis. 4, 608–616. https://doi.org/10.3978/j.issn.2072-1439.2012.10.07.

Sun, M., Brady, R.D., Wright, D.K., Kim, H.A., Zhang, S.R., Sobey, C.G., Johnstone, M.R., O'Brien, T.J., Semple, B.D., McDonald, S.J., Shultz, S.R., 2017. Treatment with an

interleukin-1 receptor antagonist mitigates neuroinflammation and brain damage after polytrauma. Brain Behav. Immun. 66, 359–371. https://doi.org/10.1016/j. bbi.2017.08.005.

Tapp, Z.M., Cornelius, S., Oberster, A., Kumar, J.E., Atluri, R., Witcher, K.G., Oliver, B., Bray, C., Velasquez, J., Zhao, F., Peng, J., Sheridan, J., Askwith, C., Godbout, J.P., Kokiko-Cochran, O.N., 2022. Sleep fragmentation engages stress-responsive circuitry, enhances inflammation and compromises hippocampal function following traumatic brain injury. Exp. Neurol. 353, 114058 https://doi.org/10.1016/j. expneurol.2022.114058.

Tapp, Z.M., Kumar, J.E., Witcher, K.G., Atluri, R.R., Velasquez, J.A., O'Neil, S.M., Dziabis, J.E., Bray, C.E., Sheridan, J.F., Godbout, J.P., Kokiko-Cochran, O.N., 2020. Sleep disruption exacerbates and prolongs the inflammatory response to traumatic brain injury. J. Neurotrauma 37, 1829–1843. https://doi.org/10.1089/ neu.2020.7010.

Tapp, Z.M., Ren, C., Palmer, K., Kumar, J., Atluri, R.R., Fitzgerald, J., Velasquez, J., Godbout, J.P., Sheridan, J.F., Kokiko-Cochran, O.N., 2023. Divergent spatial learning, enhanced neuronal transcription, and blood-brain-barrier disruption develop during recovery from post-injury sleep fragmentation. Neurotrauma Reports 4.

Torres-Platas, S.G., Cruceanu, C., Chen, G.G., Turecki, G., Mechawar, N., 2014. Evidence for increased microglial priming and macrophage recruitment in the dorsal anterior cingulate white matter of depressed suicides. Brain Behav. Immun. 42, 50–59. https://doi.org/10.1016/j.bbi.2014.05.007.

Town, T., Nikolic, V., Tan, J., 2005. The microglial "activation" continuum: from innate to adaptive responses. J. Neuroinflammation 2, 24. https://doi.org/10.1186/1742-2094-2-24.

Walker, F., Nilsson, M., Jones, K., 2013. Acute and chronic stress-induced disturbances of microglial plasticity, phenotype and function. Curr. Drug Targets 14, 1262–1276. https://doi.org/10.2174/13894501113149990208.

Ward, C.P., McCarley, R.W., Strecker, R.E., 2009. Experimental sleep fragmentation impairs spatial reference but not working memory in Fischer/Brown Norway rats. J. Sleep Res. 18, 238–244. https://doi.org/10.1111/j.1365-2869.2008.00714.x.

Wickwire, E.M., Williams, S.G., Roth, T., Capaldi, V.F., Jaffe, M., Moline, M., Motamedi, G.K., Morgan, G.W., Mysliwiec, V., Germain, A., Pazdan, R.M., Ferziger, R., Balkin, T.J., MacDonald, M.E., Macek, T.A., Yochelson, M.R., Scharf, S. M., Lettieri, C.J., 2016. Sleep, sleep disorders, and mild traumatic brain injury. What we know and what we need to know: findings from a national working group. Neurotherapeutics 13, 403–417. https://doi.org/10.1007/s13311-016-0429-3.

Witcher, K.G., Bray, C.E., Chunchai, T., Zhao, F., O'Neil, S.M., Gordillo, A.J., Campbell, W.A., McKim, D.B., Liu, X., Dziabis, J.E., Quan, N., Eiferman, D.S., Fischer, A.J., Kokiko-Cochran, O.N., Askwith, C., Godbout, J.P., 2021. Traumatic brain injury causes chronic cortical inflammation and neuronal dysfunction mediated by microglia. J. Neurosci. 41, 1597–1616. https://doi.org/10.1523/ JNEUROSCI.2469-20.2020.

Wohleb, E.S., Fenn, A.M., Pacenta, A.M., Powell, N.D., Sheridan, J.F., Godbout, J.P., 2012. Peripheral innate immune challenge exaggerated microglia activation, increased the number of inflammatory CNS macrophages, and prolonged social withdrawal in socially defeated mice. Psychoneuroendocrinology 37, 1491–1505. https://doi.org/10.1016/j.psyneuen.2012.02.003.

Woodburn, S.C., Bollinger, J.L., Wohleb, E.S., 2021. Synaptic and behavioral effects of chronic stress are linked to dynamic and sex-specific changes in microglia function and astrocyte dystrophy. Neurobiol. Stress 14, 100312. https://doi.org/10.1016/j. ynstr.2021.100312.

Woodcock, T., Morganti-Kossmann, M.C., 2013. The role of markers of inflammation in traumatic brain injury. Front. Neurol. 4 https://doi.org/10.3389/fneur.2013.00018.

Wu, S., Zou, M.H., 2020. AMPK, mitochondrial function, and cardiovascular disease. Int. J. Mol. Sci. 21, 1–34. https://doi.org/10.3390/IJMS21144987.

Xu, W., Li, T., Gao, L., Zheng, J., Yan, J., Zhang, J., Shao, A., 2019. Apelin-13/APJ system attenuates early brain injury via suppression of endoplasmic reticulum stress-associated TXNIP/NLRP3 inflammasome activation and oxidative stress in a AMPK-dependent manner after subarachnoid hemorrhage in rats. J. Neuroinflammation 16, 247. https://doi.org/10.1186/s12974-019-1620-3.

Xue, F., Du, H., 2021. TREM2 mediates microglial anti-inflammatory activations in Alzheimer's disease: lessons learned from transcriptomics. Cells 10, 321. https://doi. org/10.3390/cells10020321.

Zhang, Y., Chen, K., Sloan, S.A., Bennett, M.L., Scholze, A.R., O'Keeffe, S., Phatnani, H.P., Guarnieri, P., Caneda, C., Ruderisch, N., Deng, S., Liddelow, S.A., Zhang, C., Daneman, R., Maniatis, T., Barres, B.A., Wu, J.Q., 2014. An RNA-sequencing transcriptome and splicing database of glia, neurons, and vascular cells of the cerebral cortex. J. Neurosci. 34, 11929–11947. https://doi.org/10.1523/ JNEUROSCI.1860-14.2014.

Zyśk, M., Clausen, F., Aguilar, X., Sehlin, D., Syvänen, S., Erlandsson, A., 2019. Long-term effects of traumatic brain injury in a mouse model of Alzheimer's disease. J. Alzheim. Dis. 72, 161. https://doi.org/10.3233/JAD-190572.